UNIVERSITY OF CALIFORNIA

SANTA CRUZ

Fluvial Total Mercury and Methylmercury in the Napa River Watershed: An Agricultural Impact Assessment

A thesis submitted in partial satisfaction

of the requirements for the degree of

MASTER OF SCIENCE

in

MICROBIOLOGY AND ENVIRONMENTAL TOXICOLOGY

by

Travis J. Esquivel

June 2024

The Thesis of Travis Esquivel

is approved:

Professor Chad Saltikov, Chair

Professor Donald Smith

Professor Peter Weiss

Peter Biehl

Vice Provost and Dean of Graduate Studies

TABLE OF CONTENTS

Page

LIST OF FIGURES

Page

Fluvial Total Mercury and Methylmercury in the Napa River Watershed: An Agricultural Impact Assessment

Travis J. Esquivel

Abstract

Agricultural sulfur loading to vineyard soils has been reported to drive *in situ* mercury (Hg) methylation via microbes (with the *hgcAB* gene cluster) using sulfate in their metabolic process as an electron acceptor whereby they interconvert Hg to toxic methylmercury (MeHg). The Napa Valley, famous for world-renowned wines, is an ideal landscape to study the impact of sulfur loads potentially increasing MeHg concentrations in soils and fluvial waters. Fluvial system MeHg production is largely understudied. The goal is to characterize Hg abundance in vineyard irrigation and effluent waters, as well as the Napa River, that discharge into the San Pablo Bay critical wildlife habitat where bioaccumulation and biomagnification occur. Surface waters were collected and analyzed for: total mercury (THg), MeHg, dissolved organic carbon (DOC), sulfate (SO_4^{2-}), and total suspended solids (TSS) during the rainy season of 2022/2023. Hg species were found in low concentrations - THg (0.53 - 20.09 ng/L, $\bar{x}$ = 4.90 ng/L), MeHg (0.01 - 0.29 ng/L, $\bar{x}$ = 0.10 ng/L) despite high [SO_4^{2-}] (7.58 - 192.08 mg/L, $\bar{x}$ = 40.80) clearly indicating the agricultural signal. Positive THg and DOC correlations were noted in vineyard and background sites (R^2 = 0.53 and R^2 = 0.96, respectively) in the dissolved fraction. Agrarian SO_4^{2-} loading was not associated with elevated [MeHg] in fluvial waters. MeHg production in fluvial systems is complex with many geochemical and environmental controls governing MeHg fate and requires further investigation to resolve unknowns.

Acknowledgements

Peter Weiss-Penzias

Nettie Calvin

Eve-Lyn S. Hinkley

Carl Lamborg

Douglas Castro

1. Introduction

Mercury (Hg) is a neurotoxin in humans and wildlife that has brought upon fish consumption advisories, especially regarding subsistence fishing (San Francisco Regional Water Quality Control Board, 1995; California Department of Public Health, Office of Environmental Hazard Assessment, EPA). A wide range of neurological, renal, and gastrointestinal systems symptoms are produced from toxic levels of Hg exposure (Kolipinski et al., 2020; Alpert et al., 2013). Human and wildlife Hg exposure concerns are primarily related to the organometallic form, methylmercury (MeHg). Hg species typically found in the environment are inorganic, however (Hsu-Kim et al., 2018) elemental and inorganic Hg species are routinely altered to the organometallic form. These transformations are facilitated through metabolic processes of anaerobic microorganisms including iron- and sulfate-reducing bacteria (SRB) found in soils and sediments (e.g. *Desulfovibrio desulfuricans, Desulfobulbus proprionicus*) (Kolipinski et al., 2020; Frohne et al., 2012; Schaefer et al., 2011). Deltaproteobacteria, Clostridia, and Methanomicrobia are some of the main strains performing methylation (Gilmour et al., 2011; Ranchou-Peyruse et al., 2009; Yu et al., 2013). The most studied methylators are SRB, which produce energy by using sulfate as an electron acceptor (Luo et al., 2023; Compeau and Bartha, 1985). SRB Hg bio-methylation was examined (Acha et al., 2011) in periphyton to determine correlations between SRB abundance and Hg2+ methylation capacity. Acha et al., 2011 states “a very linear correlation” was discovered between net MeHg production and Desulfobacteraceae abundance suggesting Desulfobacteraceae were the most crucial SRB group in MeHg production (Acha et al., 2011). These microbes exist in freshwater environments, and reproduce in anoxic zones e.g., stratified water column, saturated soils, benthic sediments, and periphyton biofilms (Neal-Walthall et al., 2022; Luo et al., 2023). These environmental settings provide the most common pathway for MeHg production via microorganismal Hg methylation (Luo et al., 2023; Bravo and Cosio, 2020). While aforementioned bacteria have been identified as main contributors in the methylation process

(Frohne et al., 2012), certain MeHg production mechanisms are poorly understood. Hg redox state plays a major role in eventual Hg species fate. More knowledge regarding microbes' ability to oxidize elemental Hg to Hg (II) making subsequent methylation possible (Yu and Barkay, 2022) is needed. The most recent discoveries, about a decade ago, involved *hgcAB* gene identification (Parks et al., 2013; Yu and Barkay, 2022). The discovery of Hg methylation genes (*hgcAB*) provided a significant contribution in understanding the encoded protein functions and molecular methylation mechanisms (Yu and Barkay, 2022). However, much is left to decrypt as the minutia of intracellular gene process is still unclear (Cooper et al., 2020). Furthermore, microbial physiological advantages and the mechanism of evolutionary adaptation regarding Hg methylation (Yu and Barkay, 2022) remain a mystery hidden in the dark anoxic soils where these microbes reside. Reducing environments are typically characterized by low pH in which microbial methylation is favored (Barkay and Wagner-Döbler, 2005). In addition to microbes and abiotic processes, the potential of hydrogen (pH) and DOC concentrations in water strongly influence Hg methylation in aquatic environments, (kopiliski et al., 2020; UNEP, 2013; Barkay and Wagner-Döbler, 2005) and function as geochemical controls. Hg speciation, solubility, mobility, and aquatic environment toxicity are all affected by the strong interaction between DOC and Hg (Ravichandran, 2003). DOC can inhibit methylation by organo-metallic complexation which reduces the amount of available inorganic Hg for methylation. Conversely, DOC can enhance methylmercury generation in some environments by stimulating microbial growth (Ravichandran, 2003).

The aquatic environmental settings described above are home to fish that bioaccumulate MeHg through their diet (Hall et al., 1997) and MeHg is the primary bioaccumulative Hg species accounting for over 95% found in fish (Bloom, 1992). Biomagnification occurs up the food chain as lower trophic level species are consumed by higher trophic level predators. The highest trophic level, final consumers, include humans and have the greatest “body burdens”

of MeHg (Kopliliski et al., 2020). Eating fish containing methylmercury is the most common way people are exposed to mercury in the United States (EPA).

Elevated levels of Hg in fluvial waters have been identified by other researchers downstream from legacy Hg mining operations and agricultural land usage (Kolipinski et al., 2020; Domagalski, 2001). Legacy Hg mining operations in this geologic province provide insight regarding the presence and extent of potential mercury deposits in the watershed. Agricultural land usage has been shown to impact MeHg abundance and production (Rogers, 1976; Domagalski, 2001; Marvin-DiPasquale et al., 2014). Napa Valley's agrarian landscape is a good place to characterize fluvial Hg concentrations. This is due in part to the physical structure of the valley, agricultural land usage, and geologic Hg abundance. The Napa River serves as a highway for fluvial chemical transport and provides a useful matrix for analysis. It flows over 55 miles through the valley floor from its headwaters in Calistoga to its drainage basin in the San Pablo Bay critical wildlife habitat. These critical wildlife habitat wetlands have been shown to contain high trophic level species with elevated Hg concentrations (Kolipinski et al., 2020). Wetlands like this critical habitat are ideal environmental settings for inorganic Hg methylation. Characterized by anoxic soils subjected to sustained periods of saturation, wetlands are considered methylation "hotspots" (Hsu-Kim et al., 2018). These "hotspots" are home to the microbes that methylate *in situ* Hg (Frohne et al., 2012). Understanding Hg loading to this sensitive habitat is essential to ensure public safety. This leads to investigation of these interconnected natural and anthropogenic systems. The Napa Valley remains a largely unstudied region with respect to mercury in fluvial waters. There is poor knowledge regarding MeHg production and export to the Napa River due to the presence of vineyards elemental sulfur applications to soils as fungicides.

A knowledge gap exists regarding data on Hg presence and fate in streams and soils in the Napa Valley. The region is famous for its world-renowned grape and wine production with significant portions of agricultural land usage. Pockets of enriched geologic Hg in this

geologic province are a concern due to the high potential for methylation to occur downstream in the wetlands. A common organic farming practice is to apply elemental sulfur to vineyard soils as a fungicide to combat powdery mildew during the harvest season. This practice has been linked to increases in MeHg production (Hinkley and Matson, 2011; Driscoll et al., 2003; Driscoll et al., 2007) as the sulfur stimulates activity by SRBs in the soil. SRBs utilize sulfur and carbon in their metabolic process resulting in methyl group addition to *in situ* inorganic Hg. Transformation of inorganic Hg to organic Hg enables biological systems to readily uptake and store the pollutant.

This study aims to characterize the abundance of THg and MeHg (filtered and unfiltered), in conjunction with ancillary analytes, in fluvial waters of the Napa Valley Watershed, incorporating temporal and geospatial parameters. The suite of ancillary analytes includes dissolved organic carbon (DOC), sulfate (SO_4^{2-}), and total suspended solids (TSS). The question we attempt to answer focuses on the sulfur loading impact on MeHg generation with subsequent fluvial mobilization within the watershed as agricultural runoff. Furthermore, did temporal conditions and geographic location influence THg or MeHg concentrations under a variety of hydrologic flow states during the actively stormy year of 2023. To address this query, we sampled the Napa River at multiple sites, along with vineyard and non-vineyard ephemeral tributaries. Sample acquisition timing was determined by what other researchers have identified as seasonally dependent elevated MeHg periodicity (Conaway et al., 2003; Balogh et al., 2002). This is especially relevant in a Mediterranean climate watershed like that found in the Napa Valley where hydrologic connectivity is dictated by precipitation events.

2. Methods and Materials

In an effort to capture the elevated periodicity of MeHg, THg, and other important analytes, sampling was conducted during seasonal peak flows. Analyte concentrations are typically higher when full hydrologic connectivity is engaged during peak watershed discharge. Peak flows in the Napa River are rainfall-dominated and occur between November and early April, with the majority in December through February (CA Waterboards). The hydrologic components determining the temporal sampling factor resulted in sample sets collected in January, February, and March. Hydrologic variations between the sample sets (Figure 1) resulted in (2) “high flow” sample sets (January and March), and (1) “low flow” sample set (February). Property access to the vineyard sites in this study was enabled by preexisting relationships between Eve-Lyn S. Hinckley, University of Colorado Boulder and landowners she previously worked with through her extensive research in the Napa Valley (Hinckley and Matson, 2011; Hinckley et al., 2011; Hinckley and Matson, 2009; Hinckley et al., 2020).

Water samples were collected at ten different locations (Figure 2) in January, February, and March of 2023 - and 3 locations in December 2023. All samples were collected by walking to the edge of the water and collecting a grab sample with a gloved hand in a laminar flow region of the streams. Special care was taken to ensure sample collection avoided eddies in the streams. In January, February, and March, samples were collected from 4 Napa River locations, 4 vineyard locations, and 2 background streams. The list of Napa River sites sampled includes (arranged downgradient): Napa River 1 - headwaters (NR1), Napa River 2 - Pope St. bridge (NR2), Napa River 3 - Yountville cross (NR3), and Napa River 4 - oxbow park (NR4). For vineyard and forested background samples, the site code acronyms define the location and sample type. The first letter defines the specific vineyard (C, H, T, P), and the second and third letters define the environmental/site setting (i.e. FB = forested background, VD = vineyard ditch, or VE = vineyard effluent). The vineyard/background list is as follows (arranged downgradient): CFB, CVE, TFB, HVD, PVD, and PVE. “Paired sites” are

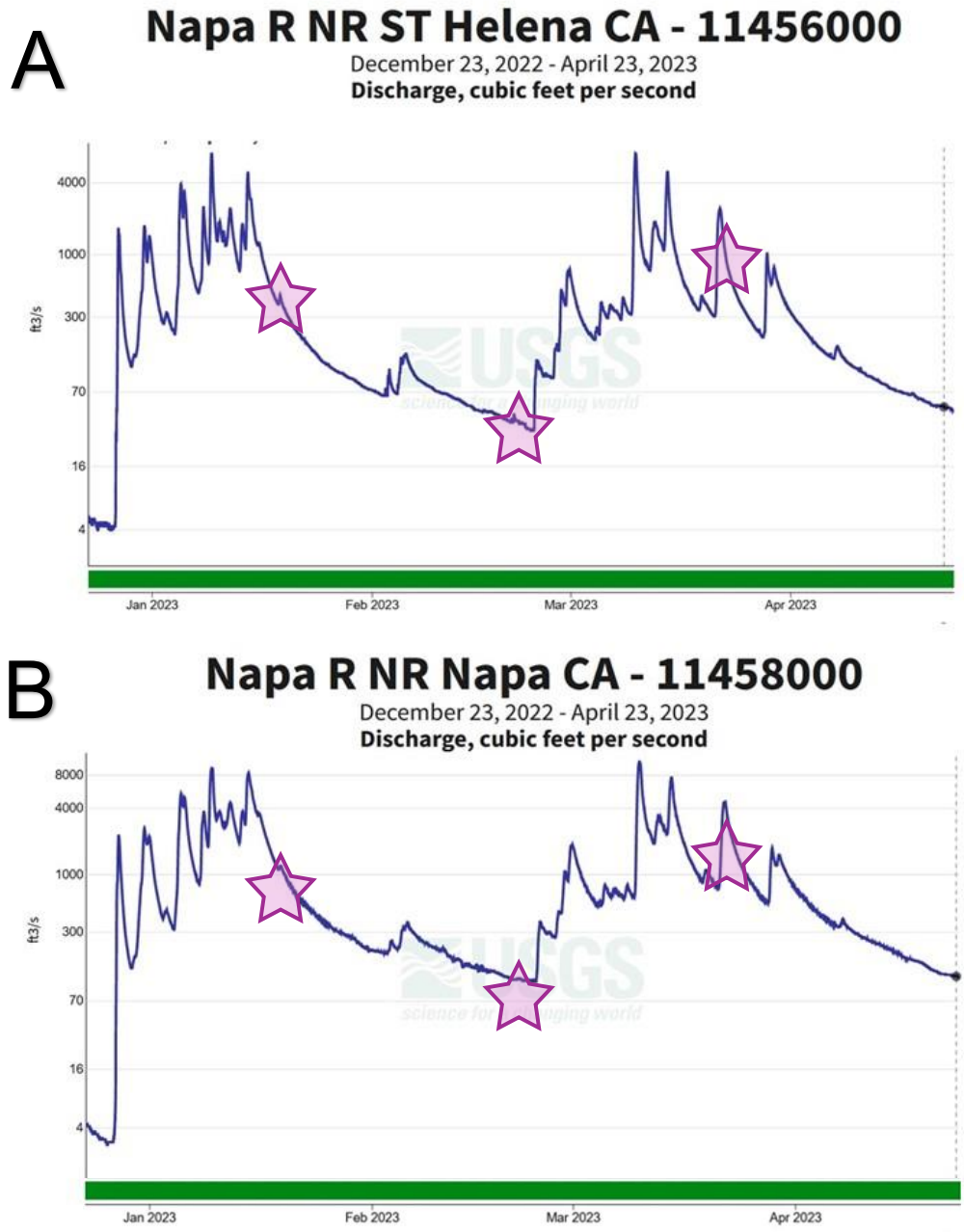

Figure 1. Napa River hydrographs from the (A) St. Helena and (B) Napa gauges. Discharge volumes are on the Y-axes with time on the X-axes. Stars indicate specific sampling times in the hydrograph. This data illuminates flow conditions during sample acquisition trips in January, February, and March of 2023 (Hydrographs provided by the USGS, waterdata.usgs.gov).

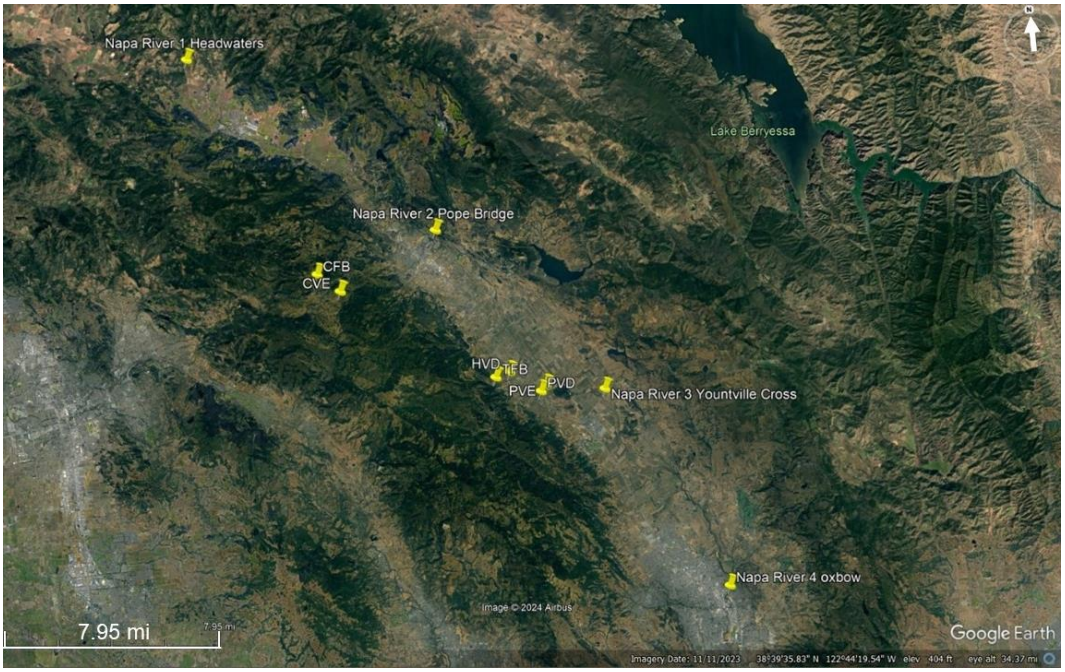

Figure 2. Google Earth image of study area (NRW) where samples were collected. The (4) river, (4) vineyard, and (2) forested background sites are indicated by yellow pushpins. Paired sites comparisons include CFB with CVE (vineyard C, forest background vs vineyard effluent), as well as TFB (Vineyard T, forested background) with HVD (vineyard H, vineyard ditch), PVD (vineyard P, vineyard ditch), and PVE (vineyard P, vineyard effluent). Vineyard sites include CVE, HVD, PVD, and PVE. Forested background sites are CFB and TFB. River sites shown with labels indicating specifics of location.

assemblages of sites that include a background and test site or sites, they include: CFB with CVE, and TFB with HVD, PVD, and PVE.

The CFB/CVE sites were selected for this study because of the engineered hillslope vineyard (CVE) that funnels all effluent to an isolated drainage culvert that has potential to serve as a point source of pollution (Figure 3). CFB is the forested background site paired to CVE, both sites are located on this property. In addition to this, the vineyard location is high in the NRW and is devoid of upgradient anthropogenic influence (Figure 4 and 5). The other vineyard sites were selected because they are subject to upgradient agricultural influences from their location in the valley floor. At site PVD/PVE, there is access to irrigation ditches draining vineyards as well as an isolated culvert that drains the PVE vineyard enabling the determination as a potential point source of pollution. Site TFB is the forested background

Figure 3. Figure shows (3) images at site CVE (vineyard C, vineyard effluent). Image A shows the vineyard hillslope. Image B shows the view looking up the hillslope illustrating the topography of the location as it funnels all runoff and effluent down to the central point at the bottom of the vineyard slope marked by metal poles and a hidden culvert beneath the boulders. Image C shows vineyard effluent draining the hillslope as a tributary with arrow indicating where sample was collected.

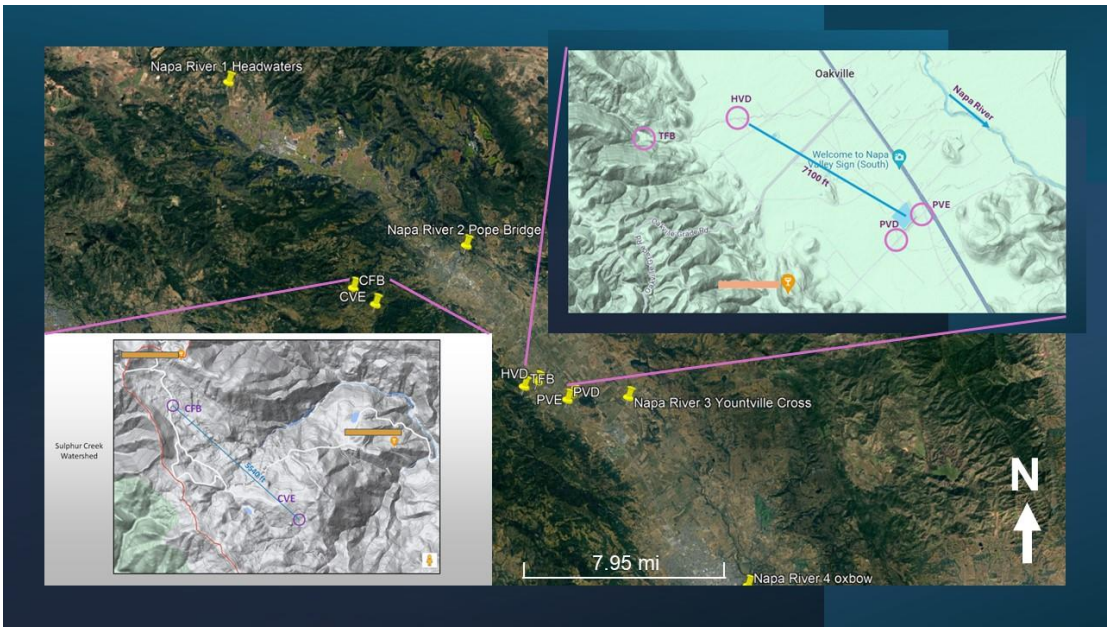

Figure 4. Aerial view of study area with insets showing paired sites and geographic relationships between sites.

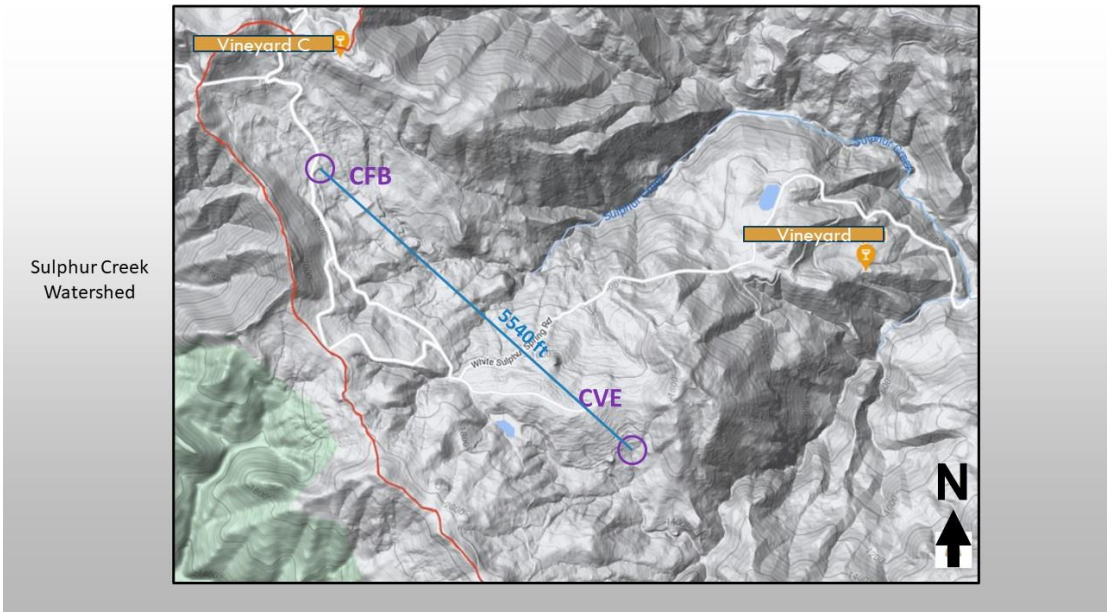

Figure 5. Topographic map view of paired sites CFB and CVE (vineyard C, forest background vs vineyard effluent) showing the geographic site location relative to each other and their location in the watershed. CVE is a vineyard effluent site and serves as a potential point source in this study. The redline indicates the upper extent of the NRW. This image provides geospatial information, absence of anthropogenic influence above sites in the watershed. (Image courtesy of Google Earth and Google Maps)

site proximal to the vineyard sites HVD, PVD, and PVE (Figure 4 and 6). The Napa River sampling sites (Figure 2 and 7) were selected to capture “big picture” dynamics of the river and transport vectors. NR1 - headwaters in Calistoga was the farthest upstream location that the general public can access. NR2 - Pope St. bridge is located before the confluence with a tributary draining Lake Hennessey. NR3 - Yountville cross is located downgradient from the valley floor vineyard locations (HVD, PVD, and PVE). Finally, NR4 - oxbow park was selected as the farthest downstream in the Napa River that is not tidally influenced.

2.1 *First flush*. An additional sample acquisition trip was made in December 2023 to collect *first flush* data. According to Sansalone and Cristina, 2004, “A *first flush* is normally defined as a disproportionate increase of particulate or dissolved materials in terms of concentration or load in the rising limb of a runoff event” (Obermann et al., 2009). Due to the physical structure and hydrologic connectivity of the watershed not all locations had flowing water

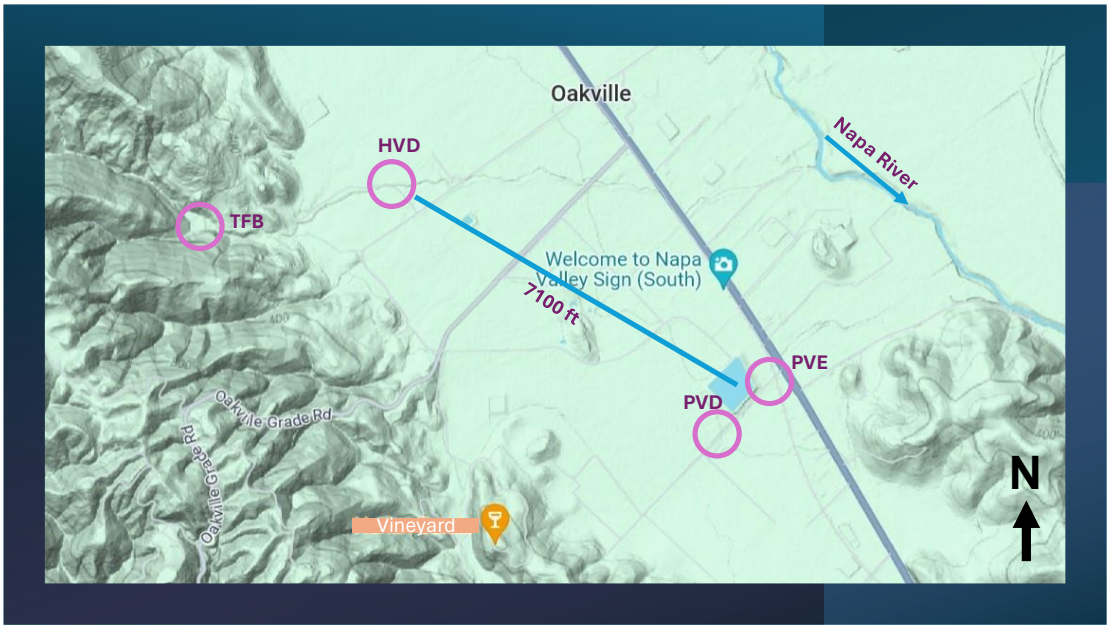

Figure 6. Topographic aerial view of paired sites TFB (vineyard T, forest background), HVD (vineyard H, vineyard ditch), PVD (vineyard P, vineyard ditch), and PVE (vineyard P, vineyard effluent). Forested background site TFB is located in the forest just above the valley floor. Vineyard sites HVD, PVD, and PVE are located on the valley floor. HVD and PVD are vineyard irrigation ditches. PVE is a vineyard effluent site and serves as a potential point source in this study. (Image courtesy of Google Earth and Google Maps)

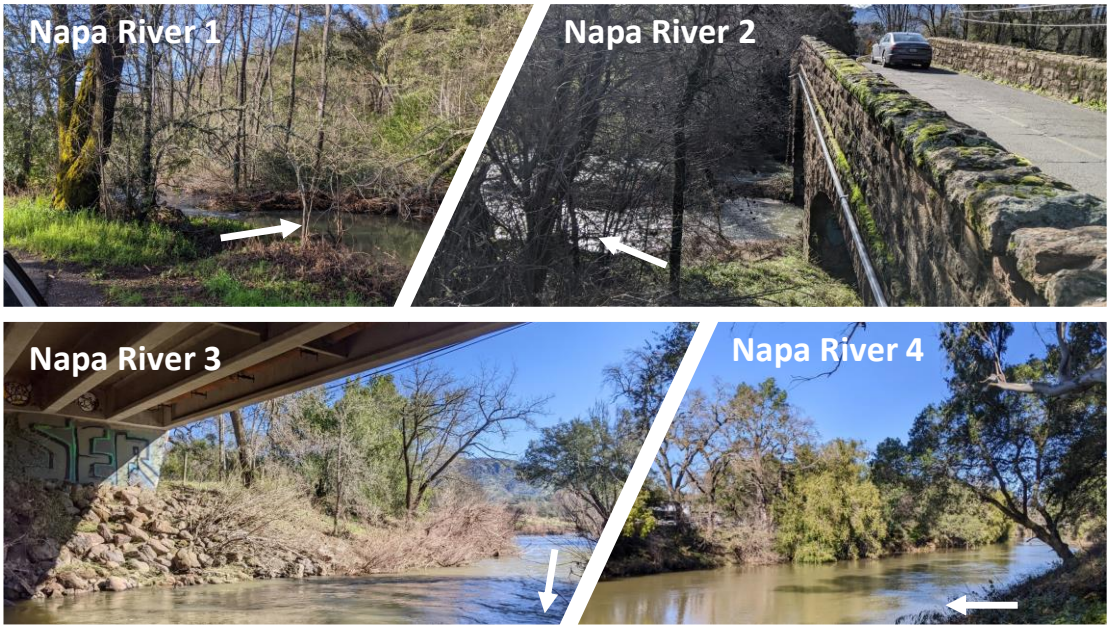

Figure 7. Image shows ground level views of the sampling sites along the Napa River (NR) with arrows indicating where samples were collected. NR1 headwaters near Calistoga, NR2 Pope Street bridge, NR3 Yountville Cross, and NR4 oxbow park near Napa.

sufficient to collect samples during this rising limb precipitation event. As such, only 3 sites provided conditions conducive to proper sample collection (CFB, CVE, and HVD).

2.2 Napa Valley Geology. The physical structure of the NRW is a northwest-trending structural and topographic depression resulting from tectonic compressional forces (Figure 8) (CA Waterboards). It encompasses 426 mi^2 (CA Waterboard) and is part of the northern Coast Ranges physiographic province (Kunkel and Upsen, 1960). Quaternary alluvial fan and valley fill deposits underlay the valley floor (Kunkel and Upsen, 1960). Upland geologic units are Jurassic to Tertiary age sedimentary and volcanic rocks that include the Sonoma Volcanics suite (Wagner et al., 2011). The voluminous Sonoma Volcanics units, as seen in Figure 9, are associated with heavy metals deposits in the region. In the 1870's, the "quicksilver" mercury mining boom occurred throughout much of the Coast Ranges. Mercury was extracted from the reddish cinnabar ore deposits. Many mining claims existed in the Mayacamas mountains that bound the western side of the Napa Valley and the mountainous region to the northeast of Calistoga (Figure 8). In California, historic Hg mining operations are the most important sources of Hg to the environment (Domagalski, 2001).

2.3 Laboratory Preparation and Analysis. Ambient low-level Hg samples are extremely susceptible to contamination from many sources. Specific modified cleaning protocols from A.G. Bravo et al., 2018 were adopted and employed for each sample acquisition trip. 250 mL amber borosilicate bottles with Teflon lined caps were used for collecting streamwater for Hg analysis. After ultra clean procedures of 24-hour Extran soap bath, followed by 24-hour bath in 10% hydrochloric acid, the bottles were filled with MilliQ water without headspace to prevent atmospheric Hg contamination. The bottles were evacuated of MilliQ immediately before filling with the sample water. Unfiltered sample collection included bottle conditioning of three rinses of streamwater before sample collection. Filtered Hg samples were processed using a peristaltic pump through a 0.45 µm filter, bottle conditioning consisted of three rinses of filtered streamwater before final sample collection. All Hg samples were then acidified with

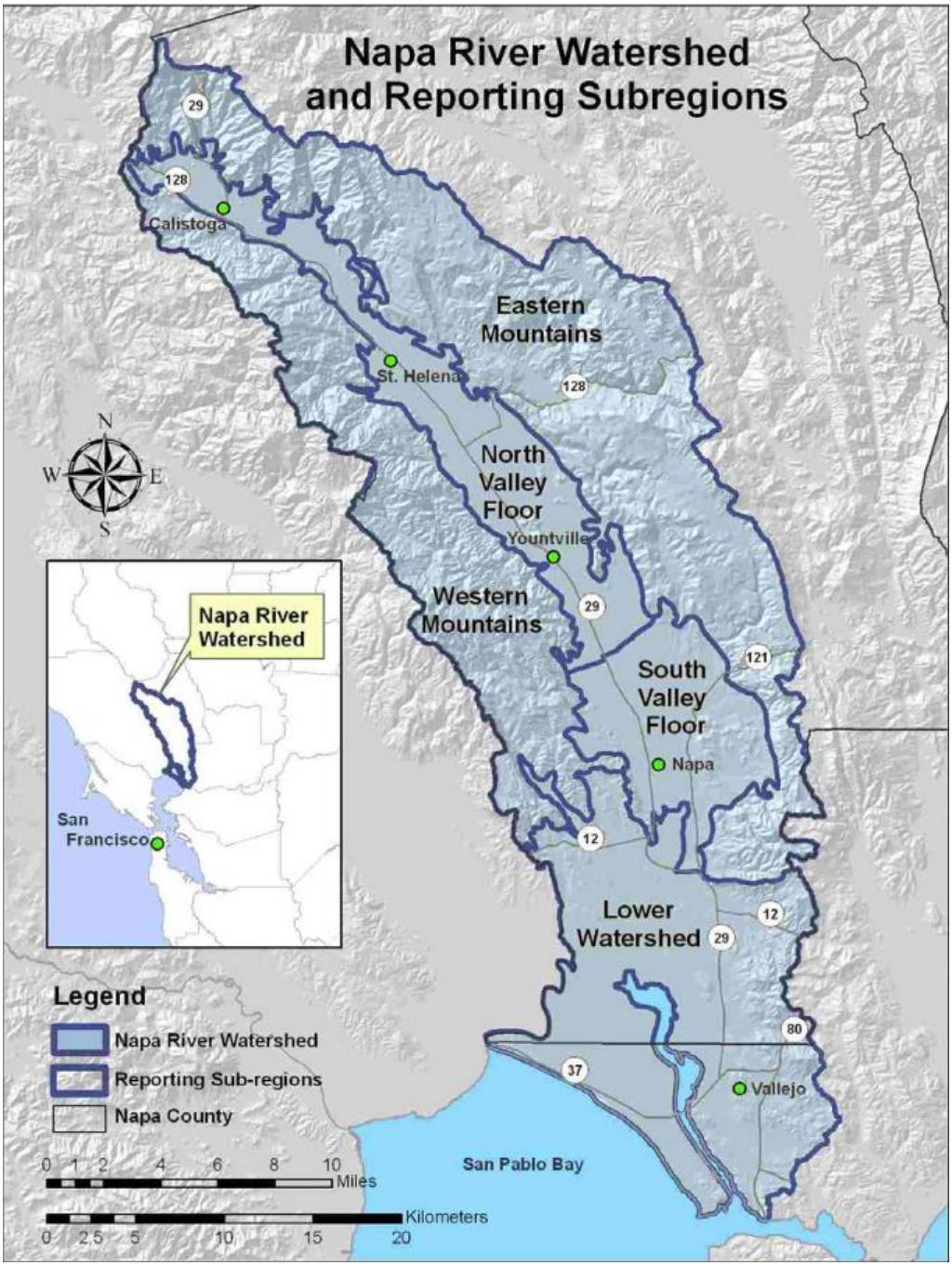

Figure 8. Aerial view of the Napa River Watershed (NRW). In the upper left of the image, the headwaters of the Napa River are just above Calistoga. The bottom of the image shows where the Napa River discharges into the San Pablo Bay Wildlife Refuge near Vallejo. (Image courtesy of napawatersheds.org)

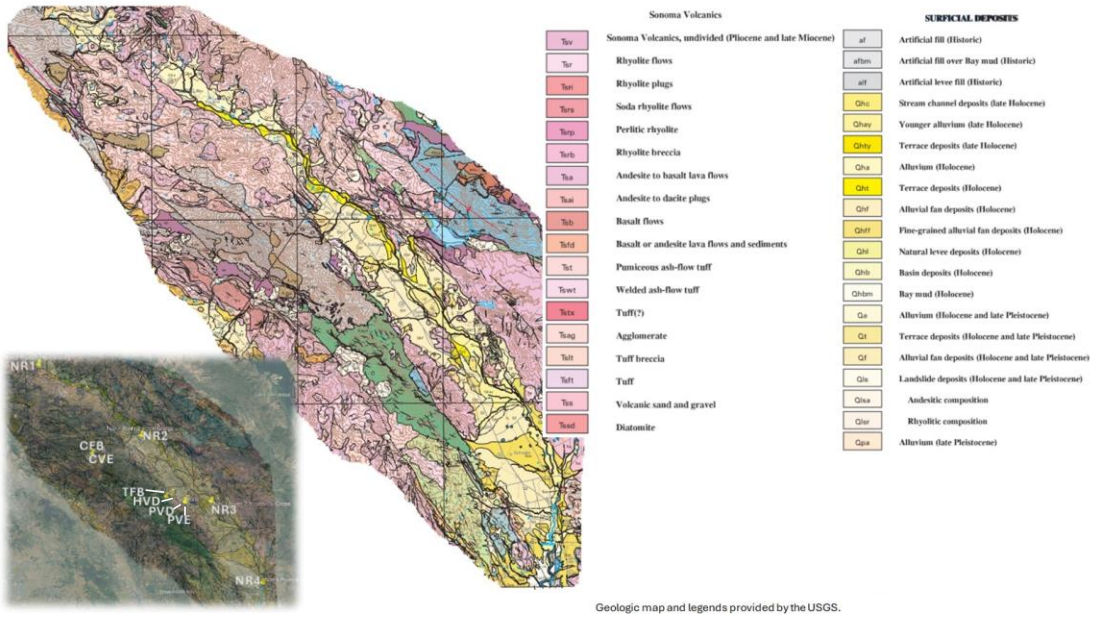

Figure 9. Section of USGS Geologic Map and Database of Eastern Sonoma and Western Napa Counties, California by Graymer et al., 2007. This cutout focuses on the Napa River Watershed. Yellowish tones indicate surficial deposits in the valley floor. The surrounding pinkish tones indicate various units within the Sonoma Volcanics suite located in the western and eastern mountain ranges that bound the watershed. Inset map image in lower left displays all sample site locations as overlay on geologic map.

250 µL of 33-36% HCl Ultrex II ultrapure reagent before being double bagged in plastic and then stored on ice.

All DOC samples were collected in 60 mL glass vials following specific cleaning protocols from Bravo et. al., 2018. Sample collection included 2 separate filtering components. The sample was first processed through the 0.45 µm filter using a battery-powered peristaltic pump and then manually using a syringe with an attached 0.2 µm Sterivex filter. The sample vials were conditioned 3 times before the sample was collected. All DOC samples were then acidified with the addition of 100 µL of 2M HCl and placed in an opaque bag on ice.

SO_4^{2-} samples were collected in 250 mL HDPE bottles and processed using the 0.45 µm peristaltic filter. Sulfate sample bottles were also conditioned 3 times before sample collection and stored on ice for preservation. Total suspended solids samples were collected in 250 mL HDPE bottles and conditioned once before collection and stored on ice.

All TSS samples were collected in 250 mL clear HDPE bottles. Samples were collected by walking to the edge of the water and collecting a grab sample with a gloved hand in a laminar flow region of the streams. Special care was taken to ensure sample collection avoided eddies in the streams. Sample collection consisted of two bottle conditioning rinses with streamwater and subsequent sample collection. Analysis was performed within 1-2 days of acquisition.

THg analyses, filtered and unfiltered, were performed by Cold Vapor Atomic Fluorescence Spectrometry (CVAFS) using bromine monochloride (BrCl) oxidation and Tin (II) chloride ($SnCl_2$) reduction with dual amalgamation on a Tekran 2600 (Bloom and Crecelius, 1983; Bloom and Fitzgerald, 1988). EPA Method 1631E (U.S. EPA, 2002) was employed and the method detection limit (MDL) of 0.18 ng/L was determined by calculating 3X the standard deviation of the reagent blank from each analysis day. The instrument was calibrated using a five-point calibration curve. All THg analyses included (5) BrCl method blanks in each analytical run - measured before and after standards. Calibration verifications were included after every 4 samples to resolve instrumental drift.

MeHg measurements were made after the distillate extraction procedure, followed by an aqueous phase ethylation, purge and trap, isothermal GC separation, and CVAFS detection (Bloom, 1989; Horvat et al., 1993; Liang et al., 1994; Bloom and von der Geest, 1995). The distillation process setup required the use of Teflon distillation bottles filled with 50 mL of streamwater, 1 mL 9M sulfuric acid, and 0.212 µL potassium chloride. The bottles were purged with nitrogen (N_2) gas at a rate of 60 mL/min while placed in a heat block for 4 hours where they were connected to receiving Teflon bottles partially submerged in an ice bath to improve distillate recovery volumes. The distillate recovered was then partitioned into (2) 10 mL aliquots which were analyzed the following day. Before instrumental analysis, the aqueous phase ethylation step is performed on the 10 mL distillate aliquots by addition of 20 µL ascorbic acid, 40 µL acetate buffer, and ~20 µL sodium tetraethyl borate. The combined

sample solutions are then vigorously shaken for 2 minutes and let to sit for 2 hours before measurement by the instrument. The MDL for this method is 0.01 ng/L as determined by calculating 3X the standard deviation of the reagent blank from each analysis day. The instrument was calibrated using a five-point calibration curve. A total of 5 ethylation method blanks were included in each analytical run and were measured before and after standards. Calibration verifications measurements were performed after every 6 aliquots to account for instrumental drift.

SO_4^{2-} samples were sent to the University of Colorado, Boulder for analysis. The samples were analyzed via a Metrohm 930 Compact Ion Chromatography Flex. This performs single-channel ion chromatography using an anion column. The MDL for this method was calculated at 0.94 mg/L by using 3X the SD of the field blanks.

DOC samples were sent to the University of Colorado, Boulder for analysis. For DOC, carbon is analyzed via catalytic combustion via Shimadzu. The specific method is "NPOC" which stands for non-purgeable organic carbon. The water sample is acidified using 1M HCL to convert all inorganic carbon to HCO_3*(CO_2). Then it is purged with air to purge out CO_2 and only leave organic carbon in the sample. The sample is then injected into a combustion tube and subjected to catalytic oxidation where the combusted material is read using IR and mV signal. The MDL for this method is 0.05 mg/L.

TSS samples were gravimetrically determined using method EPA 160.2. A well-mixed sample is filtered through a glass fiber filter, and the residue retained on the filter is dried to constant weight at 103-105°C. The detection limit for this method is 0.5 mg/L.

Figure 10 shows the results of replicate sample analysis for four analytes (THg, MeHg, SO_4^{2-}, DOC). A total of 80 THg samples (filtered THg, unfiltered THg, field blanks, and field duplicates) were analyzed with replicate analyses of each sample equaling a total of 160

Field Duplicate Agreement

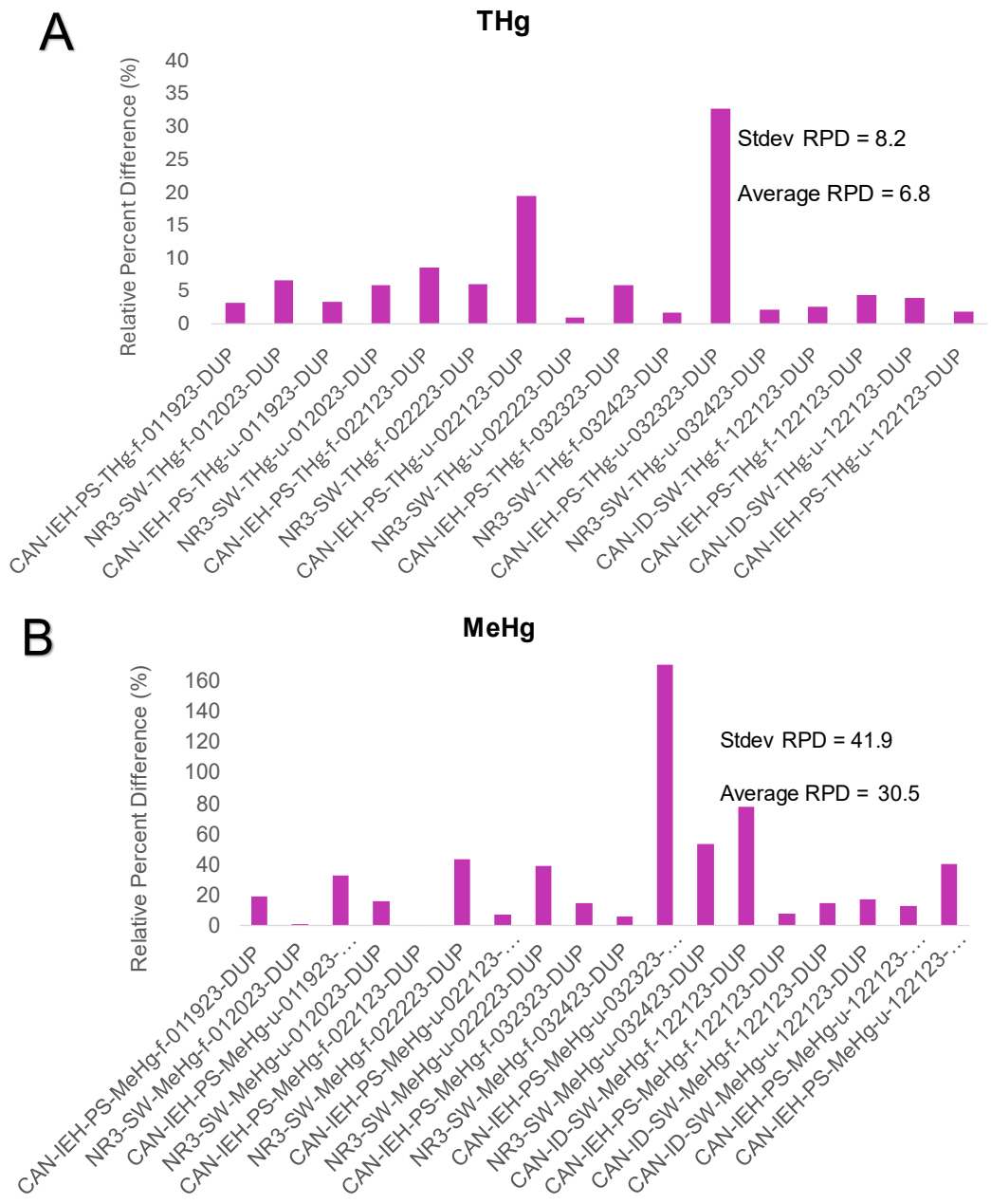

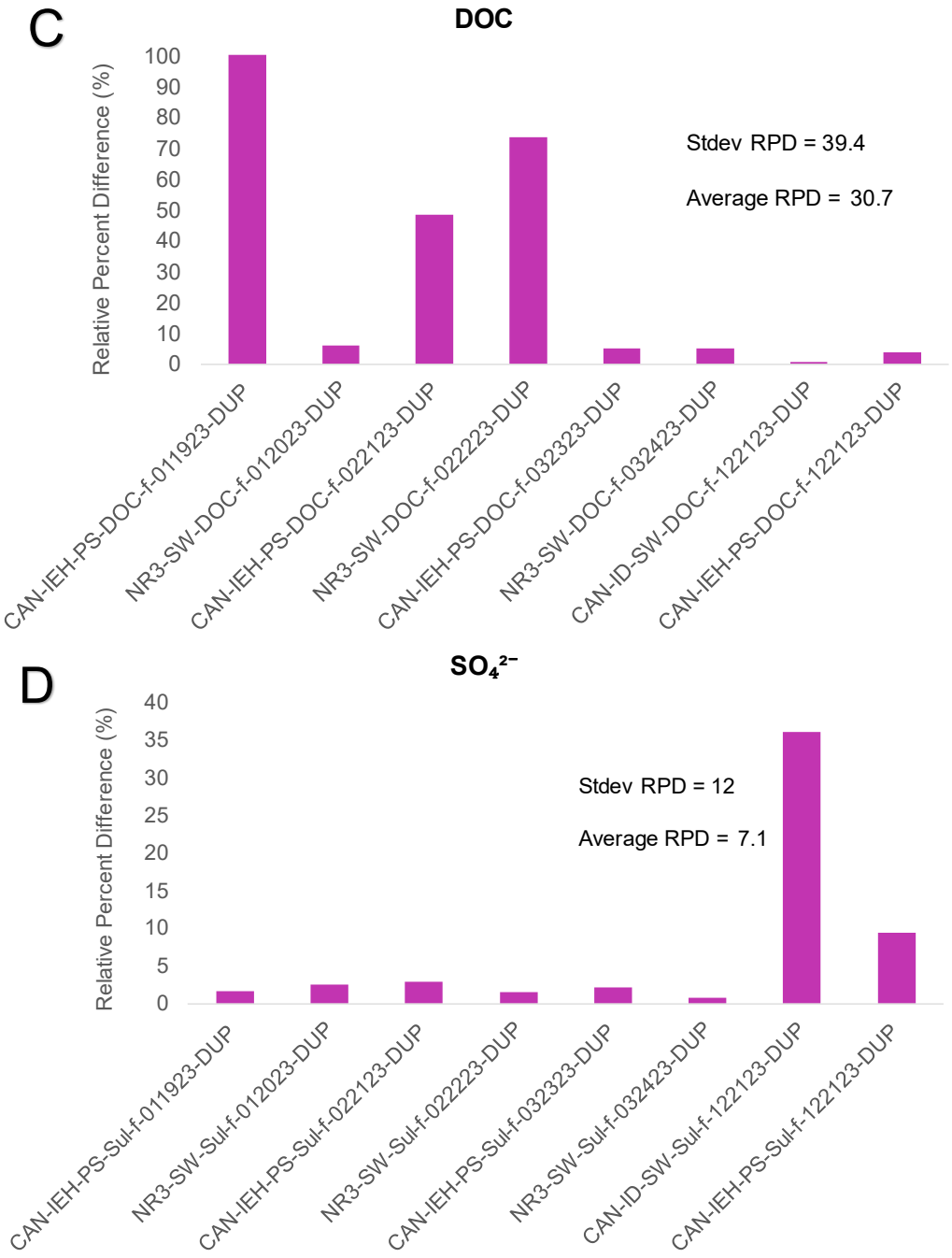

Figure 10. Field duplicates are distinct grab samples collected at the same time as regular samples. The initial sample and its duplicate sample are analyzed in the lab at the same time to determine concentration agreement between the samples. Duplicate agreement plots display the average relative percent difference (RPD) values between field duplicates of individual grab samples, and the standard deviation of the RPD for duplicate sample analyses. For each duplicate sample bar displayed n=2. Analytes include (A) THg, (B) MeHg, (C) DOC, and (D) SO_4^{2-}.

measurements (Figure 10A). THg measurements resulted in an average relative percent difference (RPD) of 6.8% with an RPD standard deviation (SD) of 8.2. A total of 85 MeHg samples (filtered MeHg, unfiltered MeHg, field blanks, and field duplicates) were analyzed with replicate analyses of each sample equaling a total of 170 measurements. MeHg measurements were reported with an average RPD of 30.5% and RPD SD of 41.9. The method of analysis for MeHg is known to include the derivatization of Hg with NaTEB, and researchers who quantify MeHg know that repeatability issues often arise. Also, many MeHg concentrations were near the MDL causing %RPD values to become large. A total of 40 SO_4^{2-} samples, which includes field blanks and duplicates, were analyzed. The results showed an average relative percent difference of 7.1% and a RPD SD of 12. A total of 40 DOC samples were analyzed, including field blanks and duplicates. The reported results had an average relative percent difference of 30.7%. DOC measurements resulted in an average RPD of 30.7% and RPD SD of 39.4.

2.4 Statistical Analysis. Statistical tests were performed on paired sites comparing the averaged results between sites (Table 1). F-Test analyses were performed to determine whether vineyard, forested background, or Napa River populations had equal or non-equal variance with the p-value set at $p<0.05$ to determine. Subsequent T-Tests were used to determine whether population means were significantly different from one another with a p-value set at $p<0.05$. All population means were not significantly different from each other, except SO_4^{2-} and DOC at TFB vs HPP. The results of the statistical analyses are for comparative purposes rather than quantitative as the data were not log transformed or normally distributed.

The correlation plots show Spearman's rank correlation as “R” in data table with associated p-value. Spearman’s R measures the strength and direction of association between two ranked variables. The closer the value is to 1 or -1 the stronger the correlation is between the variables.

Analyte	Site	Test	Result	Decision
u-THg	CFB	F-Test	0.280	(non-equal variance)
	CVE	T-Test	0.126	(means not sig different)
	TFB	F-Test	0.730	(non-equal variance)
	HPP	T-Test	0.490	(means not sig different)
u-MeHg	CFB	F-Test	0.415	(non-equal variance)
	CVE	T-Test	0.114	(means not sig different)
	TFB	F-Test	0.433	(non-equal variance)
	HPP	T-Test	0.211	(means not sig different)
Sulfate	CFB	F-Test	0.006	(equal variance)
	CVE	T-Test	0.202	(means not sig different)
	TFB	F-Test	0.299	(non-Equal variance)
	HPP	T-Test	0.033	(significantly different means)
DOC	CFB	F-Test	0.385	(non-equal variance)
	CVE	T-Test	0.078	(means not sig different)
	TFB	F-Test	0.027	(equal variance)
	HPP	T-Test	0.090	(means not sig different)
TSS	CFB	F-Test	0.650	(non-equal variance)
	CVE	T-Test	0.448	(means not sig different)
	TFB	F-Test	0.650	(non-equal varince)
	HPP	T-Test	0.448	(means not sig different)

Table 1. Statistical test results of F-Test and T-Test performed on unfiltered-Hg, SO_4^{2-}, DOC, and TSS data comparing Test versus Background samples at paired sites. Stats testing performed on paired sites, i.e. CFB with CVE (forested background vs vineyard effluent). HPP is the average of 3 vineyard sites (HVD, PVD, and PVE) compared to forested background site TFB. F-Test results inform T-Test of equal or non-equal variance in the population. T-Test result determines whether means are statistically significant ($p \leq 0.05$).

3. Results

3.1 Concentrations of Analytes by Site and by Hydrologic State. Results from the analyses of water samples taken at ten sites in the Napa Valley during 4 hydrologic states (Jan, Feb, Mar, Dec, Figure 1 and 11) are presented.

3.1.1 THg. The Napa River samples had the highest concentrations of THg as compared to background and vineyard samples. Higher concentrations were quantified in the January and March high flow sample sets (Figure 12A). The February data set clearly shows a discharge volume effect lowering the [THg]. The data shows a correlation between high [THg] with high discharge rate as the highest [THg] were seen in March when the flow was the highest (NR2 and NR3). This correlation effect does not hold true for site NR1 as it is strongly influenced by the Kimball Canyon Reservoir proximally upstream from the site. Additionally, NR1 lacks discharge volume data as there is no gauge located at the headwaters. The influence of discharge volume on [THg] is also observed in vineyard and background sites. These location types had lower [THg] than Napa River site locations (Figure 12 and 13).

Napa River THg measurements ranged from 1.39 - 20.09 ng/L with an average of 6.75 ng/L. Filtered THg concentrations ranged from 1.39 - 6.95 ng/L with a mean value of 3.89 ng/L. Unfiltered THg concentrations ranged from 2.67 - 20.09 ng/L with a mean value of 9.61 ng/L.

Vineyard and forested background THg samples ranged from 0.53 - 12.60 ng/L with a mean value of 3.05 ng/L. Filtered THg concentrations ranged from 0.53 - 11.46 ng/L with a mean value of 2.69 ng/L. Unfiltered THg concentrations ranged 0.80 - 12.60 ng/L with a mean value of 3.41 ng/L.

PVE (vineyard site P, vineyard effluent), the site furthest downgradient in the study, consistently had the lowest THg concentrations of any site in this study. This site also consistently had the highest values of SO_4^{2-}. This correlation may be the result of Hg

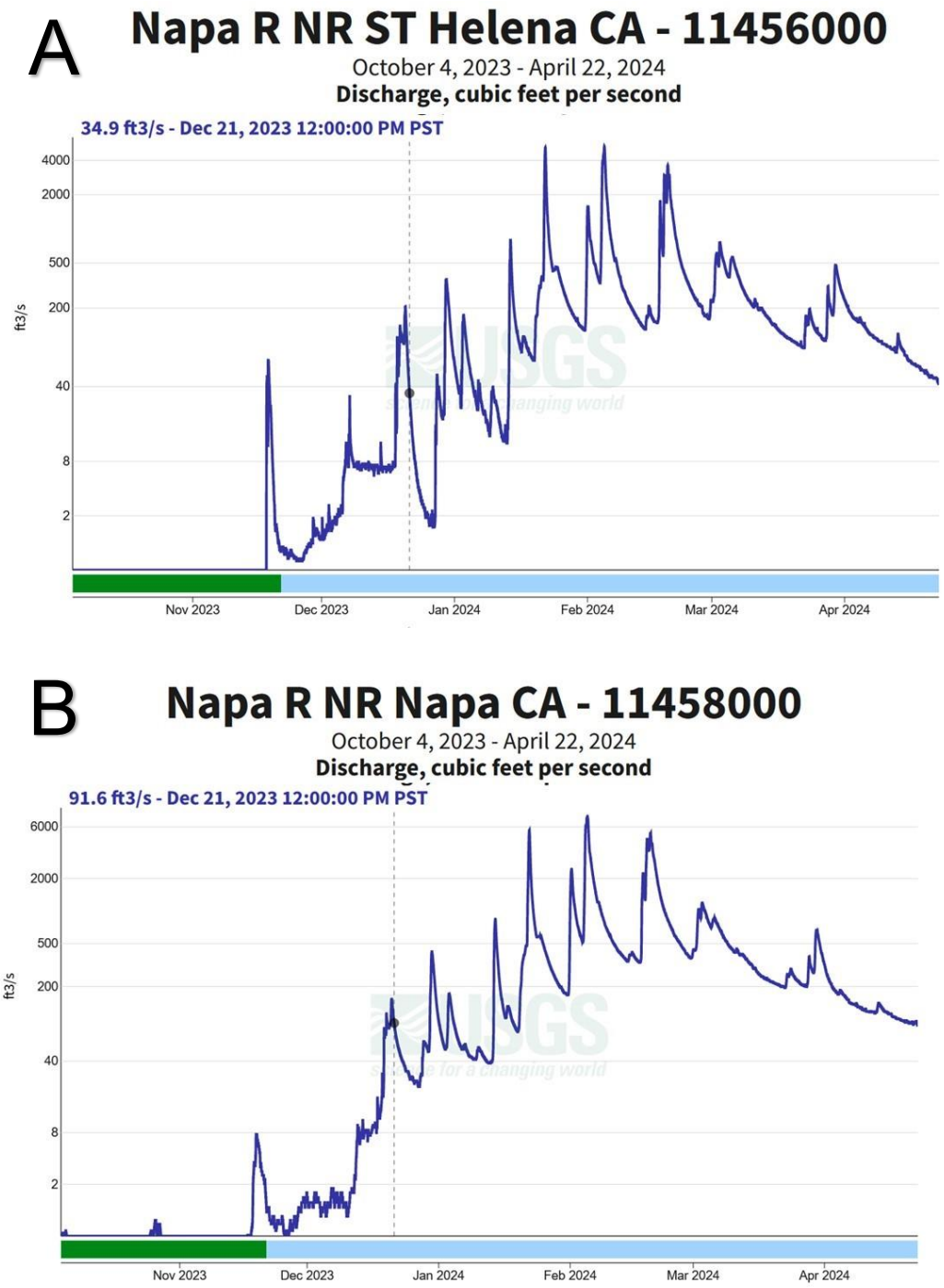

Figure 11. Napa River hydrographs of the St. Helena and Napa gauges from the *first flush* sample set collected in December 2023. Discharge volumes are on the Y-axes with time on the X-axes. Vertical dashed lines indicate the discharge rate on the day of sampling. Green bar at bottom of hydrograph indicates approved data, blue bar indicates provisional data.

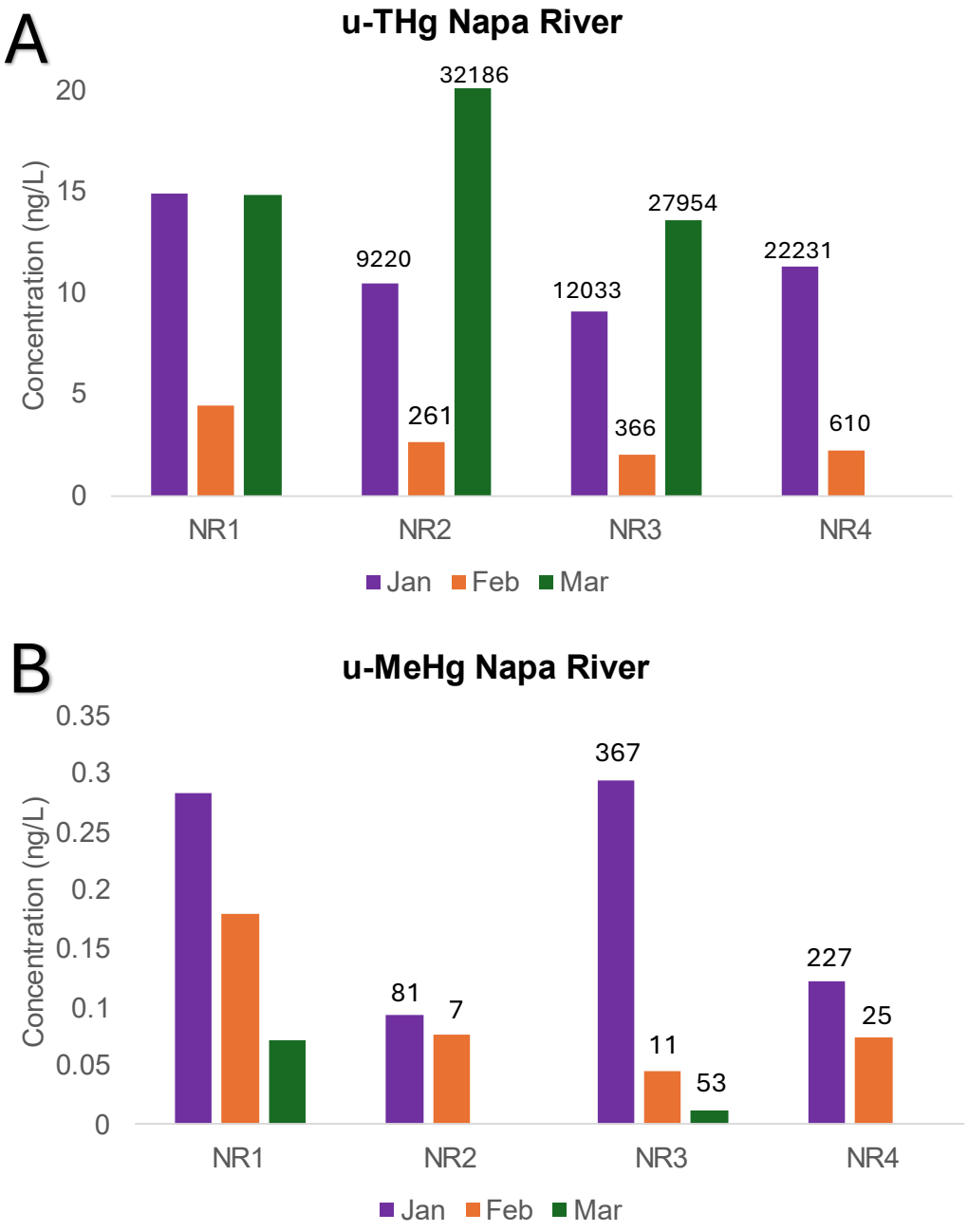

Figure 12. Napa River (A) unfiltered-THg and (B) unfiltered-MeHg measurements in units of nanograms per liter (ng/L). Daily load calculation values shown above bars are in units of milligrams per day (mg/day). Lab quantified concentrations of analytes in conjunction with iterative discharge volume calculations used to generate daily load quantities. The St. Helena and Napa River gauge stations enabled discharge volume calculations (hydrograph data for both stations seen in Figure 1). No sample data for NR2 in March due to a broken sample bottle. Riverbank sedimentation at NR4 restricted access and prohibited March sample collection. Results presented are the average of (2) replicate analyses per bar, n=1.

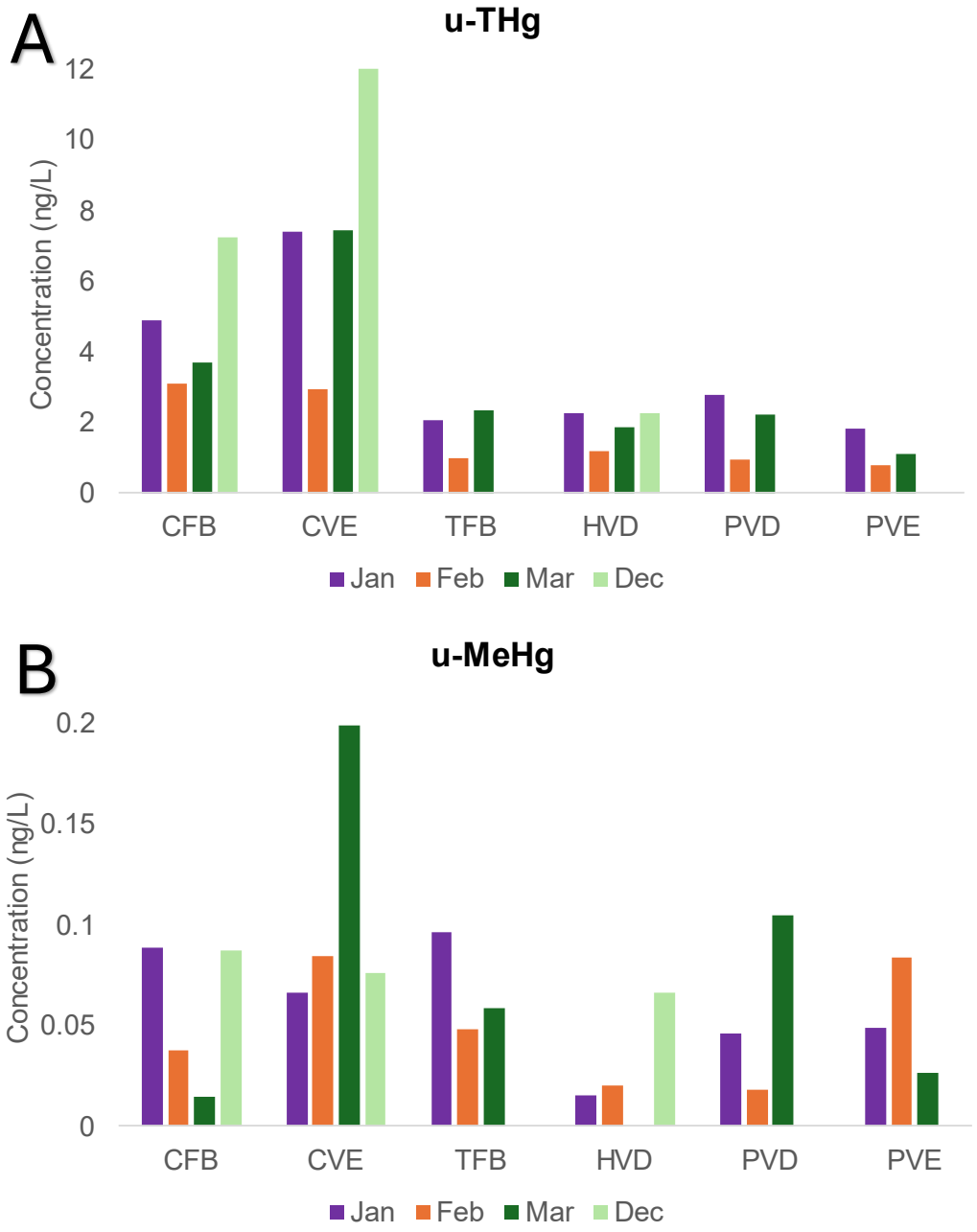

Figure 13. Vineyard (CVE, HVD, PVD, and PVE) and forested background (CFB and TFB) sites (A) unfiltered-THg and (B) unfiltered-MeHg measurements are shown in units of nanograms per liter (ng/L). X-axis shows sites arranged downgradient towards the right; each sample site has each month's result displayed. Results presented are the average of (2) replicate analyses per bar, n=1.

complex formation and subsequent immobilization. Mercury sulfate complexes are insoluble in water and may be a control on the observed Hg concentrations measured in this study.

The prevalence of agricultural SO_4^{2-} in the watershed may potentially be a factor immobilizing Hg present in soils. As such, $HgSO_4$ complexation could also be a geochemical control on Hg available for methylation and thus reduce MeHg concentrations overall (Manceau et al., 2015).

3.1.2 MeHg. As mentioned in section 3.1.1, the effect of discharge volume on analyte concentrations can be seen in the MeHg data comparing January and February sample sets (Figure 12B). All [MeHg] were higher in the January sample set versus February sample set. There were multiple complications in the March NR MeHg data set. The sample bottle for NR2 u-MeHg broke in the laboratory during a power outage refrigerator transit. Additionally, sample collection at NR4 was prohibited by river bank sedimentation resulting from historic precipitation events during early and mid-March.

Napa River MeHg samples ranged from 0.012 - 0.29 ng/L with a mean value of 0.12 ng/L. Filtered MeHg concentrations ranged from 0.046 - 0.24 ng/L with a mean value of 0.11 ng/L. Unfiltered MeHg concentrations ranged from 0.012 - 0.29 ng/L with a mean value of 0.13 ng/L.

Vineyard and forested background MeHg measurements were quantified with a range from below detection limits at 0.010 ng/L to a maximum of 0.28 ng/L with a mean value of 0.086 ng/L. Filtered MeHg concentrations ranged from 0.010 - 0.28 ng/L with a mean value of 0.076 ng/L. Unfiltered MeHg concentrations ranged from 0.014 - 0.20 ng/L with a mean value of 0.096 ng/L.

NR1 headwaters had some of the highest concentrations of MeHg in this study. Referencing the site position in the watershed we can infer that this result is due to reservoir management upstream. NR1 Headwaters is the furthest upstream in the Napa River that the public can access and is proximal to the Kimball Canyon Reservoir. Reservoirs are known sinks for

MeHg due to low flow, anoxic, and light-deprived conditions conducive to MeHg production (Hall et al., 2005). Additionally, the Kimball Canyon Reservoir is enveloped by forested lands. The environmental setting surrounding the reservoir provides ample litterfall and throughfall to elevate MeHg concentrations (Fisher and Wolfe, 2012). MeHg concentrations in underlying soils and in runoff waters that drain those soils are strongly influenced by forested riparian leaf litter areas (Balogh et al., 2002). Overall, the concentrations measured in this study were on par with other research (Tsui et al., 2009) regarding MeHg abundance in northern California fluvial systems.

3.1.3 Dissolved Organic Carbon. DOC sample measurements in this study (Figure 14 and 15) were quantified within a range of 1.20 - 10.89 mg/L with a mean value of 4.42 mg/L. Napa River samples ranged from 1.80 - 8.22 mg/L with a mean value of 3.47 mg/L. Vineyard and forested background samples ranged from 1.20 - 10.89 mg/L with a mean value of 4.90 mg/L. The highest value determined was measured at CVE with a concentration of 10.89 mg/L collected during the December *first flush* sample set. The lowest measured concentration was observed in February at the TFB site with a value of 1.20 mg/L. A statistical outlier was identified in February at site PVE (19.06 mg/L) and was removed from plots. However, if the outlier is not excluded from the data set, a trend in the February sample set showed higher [DOC] at all vineyard and forested background sites except TFB and HVD. HVD is the most proximal site to background site TFB which speaks to the similarity in their data trend, specifically in February. There is potential for DOC to be elevated in low flow conditions, but more data is needed to resolve this supposition. Beyond this supposition, there were no salient trends or patterns elucidated in the data.

Positive correlations between DOC and THg are not untypical in Hg research within fluvial waters (Lavoie et al., 2022). Both DOC and Hg are mechanistically coupled elements that should covary in natural ecosystems (Lavoie et al., 2022). Generally, DOC is viewed as a Hg vector in freshwater ecosystems at the catchment scale

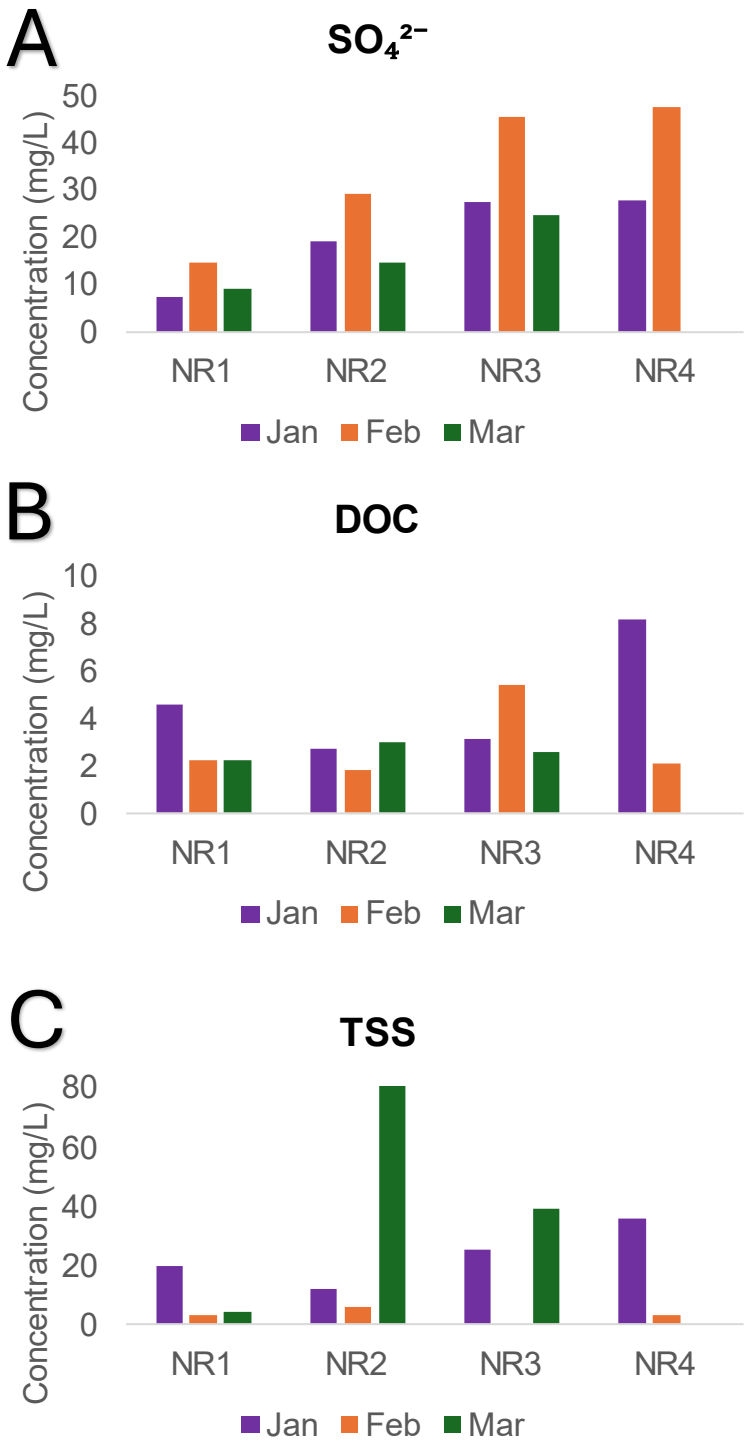

Figure 14. Ancillary analyte concentrations of SO_4^{2-} (A), DOC (B), and TSS (C) for Napa River sites (NR1, NR2, NR3, and NR4) in units of milligrams per day (mg/L) showing the results of all (3) NR sample sets. Results presented are the average of (2) replicate analyses per bar, n=1.

(Lavoie et al., 2022; Grigal, 2002; Ravichandran, 2004). The coupling between Hg and DOC has robust empirical evidence, but variations in Hg–DOC linear relationships and the causes are poorly understood (Grigal 2002; Stoken et al., 2016; Lavoie et al., 2022). Positive correlations between DOC and THg in this study were identified in the dissolved fraction at vineyard sites ($R^2 = 0.53$) with the highest correlation found at forested background sites ($R^2 = 0.956$). However, no positive correlations were made between DOC and THg in undissolved fractions. TFB consistently had the lowest DOC concentrations of any site in this study.

3.1.4 Sulfate. SO_4^{2-} sample measurements (Figure 14, 15) in this study were quantified within a range of 7.58 - 192.08 mg/L with a mean value of 40.80 mg/L. Napa River samples were quantified in a range of 7.58 - 47.74 mg/L with a mean value of 24.47 mg/L. Vineyard and forested background samples were quantified in a range of 9.71 - 192.08 mg/L with a mean value of 49.36 mg/L. The highest concentration was observed in March at the PVE site with a value of 192.08 mg/L. PVE had the highest concentrations of any site throughout the entirety of the study. The lowest concentration was measured in the Napa River at NR1 headwaters with a value of 7.58 mg/L. NR1 had the lowest values measured throughout the study.

NR1 lowest sulfate measurement was made in January. This location is not subject to vineyard farming impacts and, as such, consistently had the lowest sulfate concentrations of any site in this study.

The data have shown a clear agricultural signal influence based on geographic site position in the watershed. Higher concentrations of aqueous SO_4^{2-} draining vineyards, relative to surrounding forest/grasslands settings, were also identified by researchers investigating fungicidal Sulfur applications via stable isotopes (δ34S–SO42−) in the Napa River Watershed (Hermes et al., 2022). Sample sites in the valley floor had the highest amounts of SO_4^{2-} as

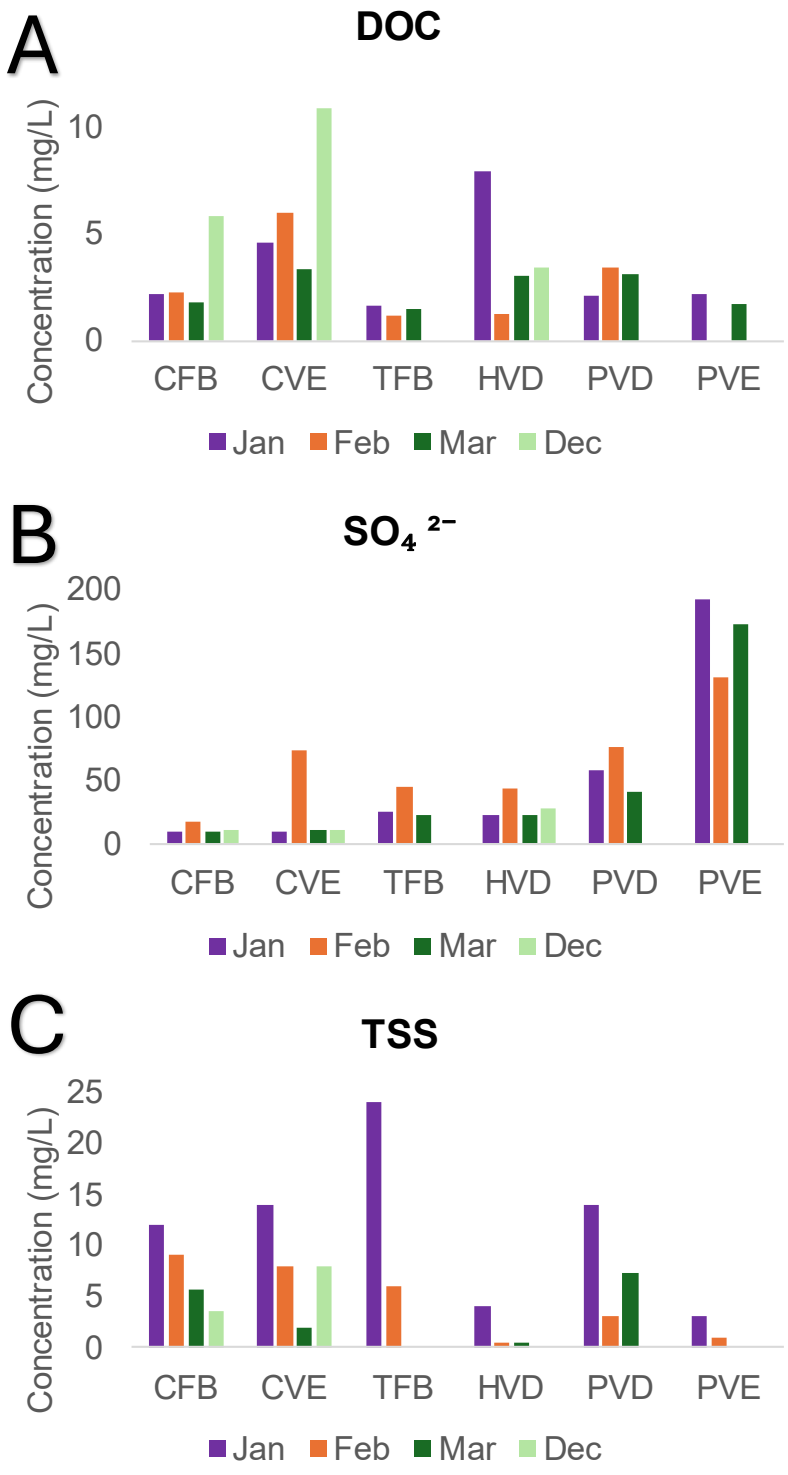

Figure 15. Ancillary analyte concentrations of (A) DOC, (B) SO_4^{2-}, and (C) TSS for vineyards (CVE, HVD, PVD, and PVE) and their paired forested background (CFB and TFB) sites shown in units of milligrams per day (mg/L).

these sites were subjected to the most anthropogenic influences. In addition to elemental sulfur use as a fungicide, ammonium sulfate $(NH_4)_2(SO_4)$ fertilizer use is another source of SO_4^{2-} increasing the overall load in the watershed. SO_4^{2-} was observed in highest concentrations during the low flow February sample set, except site PVE. PVE had slightly more SO_4^{2-} in both January and March sample sets. However, PVE consistently had the highest concentrations of SO_4^{2-} for any site in this study. PVE was 7-8X higher than the average of all other vineyard/forested background sites during the high flow sample sets collected in January and March. During the low flow sample set collected in February, PVE was over 2.5X higher than the average of all other vineyard/forested background sites. The vineyard/forested background site with the lowest SO_4^{2-} concentrations was CFB. CFB does not have any anthropogenic influence due to its elevated watershed position. Explanations for high SO_4^{2-} concentrations observed during the low flow February sample set can be attributed to the solubility of SO_4^{2-}. In high precipitation events the super solubility of SO_4^{2-} is being diluted which results in low concentrations, whereas instances of low flow results in leaching out of the fields and aqueous enrichment of SO_4^{2-}.

A clear trend in the SO_4^{2-} data was noted in the Napa River as the concentration increased steadily progressing downstream. For each sample set collected, this was the case. Regarding the high SO_4^{2-} concentration during the low flow regime, the highest concentrations of SO_4^{2-} were quantified in the February sample set. This trend is a regional signature of agricultural impact.

There are many determining factors to MeHg production (redox, pH, DOC, Fe, Cl-, and SO_4^{2-}) but high amounts of SO_4^{2-} are known to stimulate SRB activity resulting in higher MeHg production rates. However, a perplexing relationship identified by colleagues conducting research on Hg methylation rates (Weiss et al., Unpublished) in the NRW have observed the lowest methylation rates in the highest SO_4^{2-} environments.

3.1.5 Total Suspended Solids. A total of 32 total suspended solids determinations (Figure 14 and 15) were made in this study. The range of TSS for the study was 0 - 80.4 mg/L with a mean value of 11.44 mg/L. Napa River measurements were determined in a range of 0 - 80.4 mg/L with a mean value of 20.8 mg/L. Vineyard and forested background samples were determined in a range of 0 - 24 mg/L with a mean value of 6.29 mg/L. TSS data showed a general trend of higher suspended solids during higher flow rates in the watershed. NR3 in February was below the limit of detection, but broadly analyzing the data trend reveals lower loads during lower flow rates, which follows logic when considering sediment transport mechanisms. Less precipitation results in less overall transport by overland flow, entrainment, and saltation in streams. A qualitative observation can be made when referring to suspended solids as the clarity of water decreases as the suspended load increases. That said, despite lacking NR4 sample data in March, the river was seen laden with sediment resulting in turbid and murky brown water as viewed from the upper banks suggesting that a sample would have resulted in high TSS. Considering the absent-to-miniscule load at NR3 in February, and the qualitative observation at NR4 in March, then resolution becomes clearer and leads to the determination that indeed the data shows higher [TSS] with higher flow volumes. This concept is well known and reported by other fluvial researchers (Domagalski, 2001).

3.2 THg and MeHg Load Calculations. Total daily load calculations were made using hydrograph data from (2) gauge stations on the Napa River. Both the St. Helena and Napa River gauge stations were used to calculate discharge volumes of sample sites located between gauges. Lab quantified concentrations of THg and MeHg were used in conjunction with iterative discharge volume calculations to generate reported daily load quantities. The highest calculated THg load was determined at the Napa River 2 Pope st. location during March with a total of 32186 mg/day. All other calculated daily load values can be seen over their respective sample location bar in Figure 12. The highest calculated MeHg load was determined at the Napa River 3 Yountville Cross location during January with a value of 367

mg/day. Other Hg research conducted in N. California (Domagalski, 2001) resulted in observed MeHg loads in the Sacramento River of 8000, 20,000, 28,000, and 24,000 mg/day in December, January, February, and March, respectively.

3.3 Correlations and Comparisons. Correlation plots in Figures 16, 17, and 18 are displayed with data tables on plots reporting Spearman's "R" value and the associated p-value. Statistically significant correlations are denoted in bold text. Figure 16 looks at relationships with f-THg, the X-axis is the independent variable in this case (f-THg) and the Y-axis is the independent variable (f-MeHg). Most of the correlation plots had low R^2 values, which is the coefficient of determination and reflects the how much variation in the Y-variable can be explained by variation in the X-variable, however, factors important for f-THg were seen in plots A and C (Figure 16). In Figure 16A there are two site types that are positively correlated for f-THg, a little more than 44% of the variability in f-THg in the vineyards can be explained by f-MeHg. These results are potentially important as more THg may result in more MeHg. This is especially important considering the highest THg/MeHg correlation was observed in the vineyard samples suggesting that MeHg generation could be occurring to an appreciable amount in vineyard soils. In comparison, Figure 16B shows negative correlations in THg/SO_4^{2-} in all site types. This information is also important as these correlations could be a reflection of Hg complex formation which has the capacity to reduce aqueous Hg mobilization which would result in lower fluvial [Hg species]. In Figure 16C, positive correlations are observed in all site types with a couple important correlations observed in vineyard samples. More than 53% of the variability in the independent variable (f-THg) was explained by DOC abundance in Napa River samples. The correlation with the highest R^2 value in this study was between f-THg and DOC in background forest samples with over 95% of f-THg explained by DOC, and a Spearman's R value of 0.98. In Figure 16D, f-THg and TSS were weakly correlated. This result could be attributed to the fact that TSS is in the

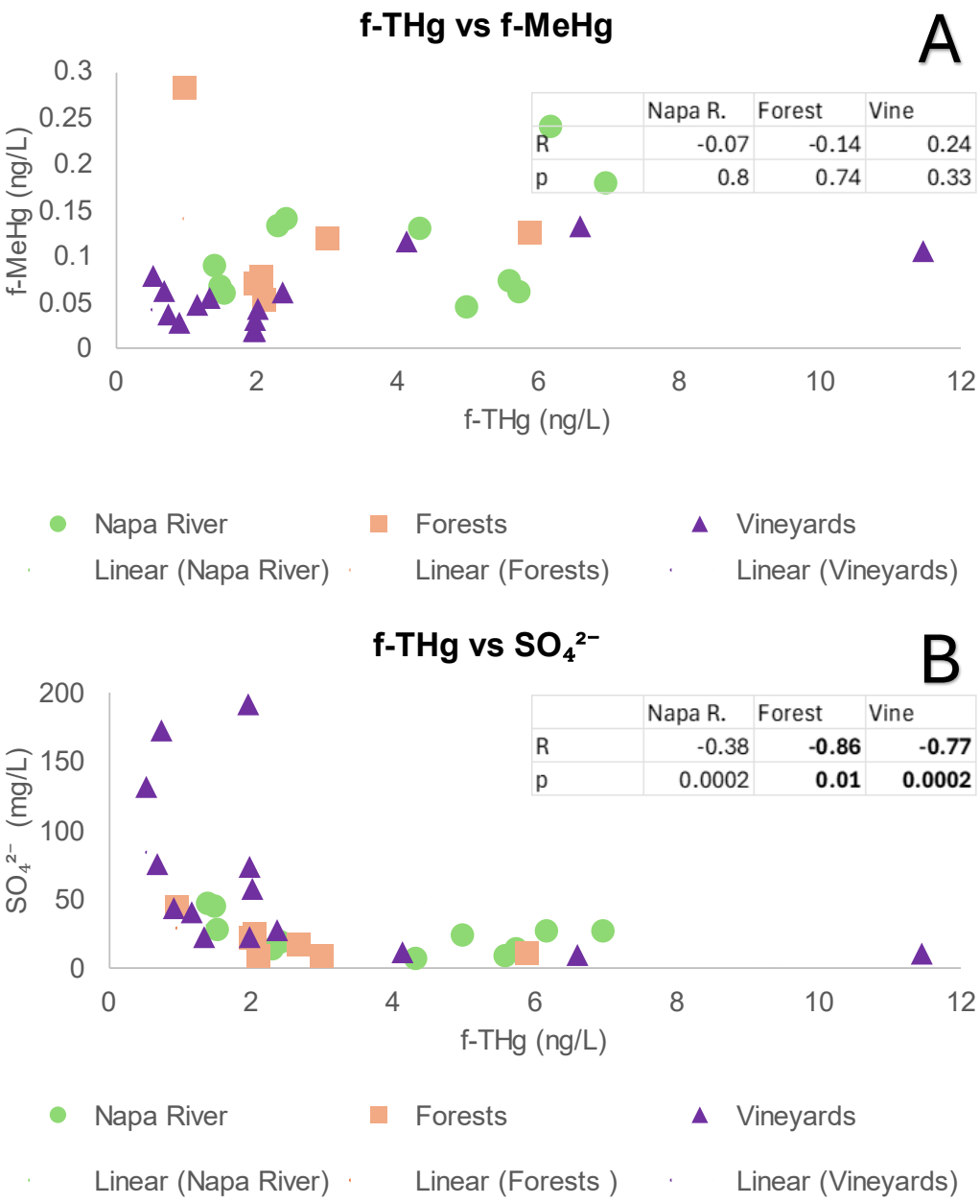
f-THg vs f-MeHg
A
f-MeHg (ng/L)
f-THg (ng/L)
Napa R. Forest Vine
R -0.07 -0.14 0.24
p 0.8 0.74 0.33
Napa River
Forests
Vineyards
Linear (Napa River)
Linear (Forests)
Linear (Vineyards)
f-THg vs SO4 2−
B
SO4 2− (mg/L)
f-THg (ng/L)
Napa R. Forest Vine
R -0.38 -0.86 -0.77
p 0.0002 0.01 0.0002
Napa River
Forests
Vineyards
Linear (Napa River)
Linear (Forests)
Linear (Vineyards)

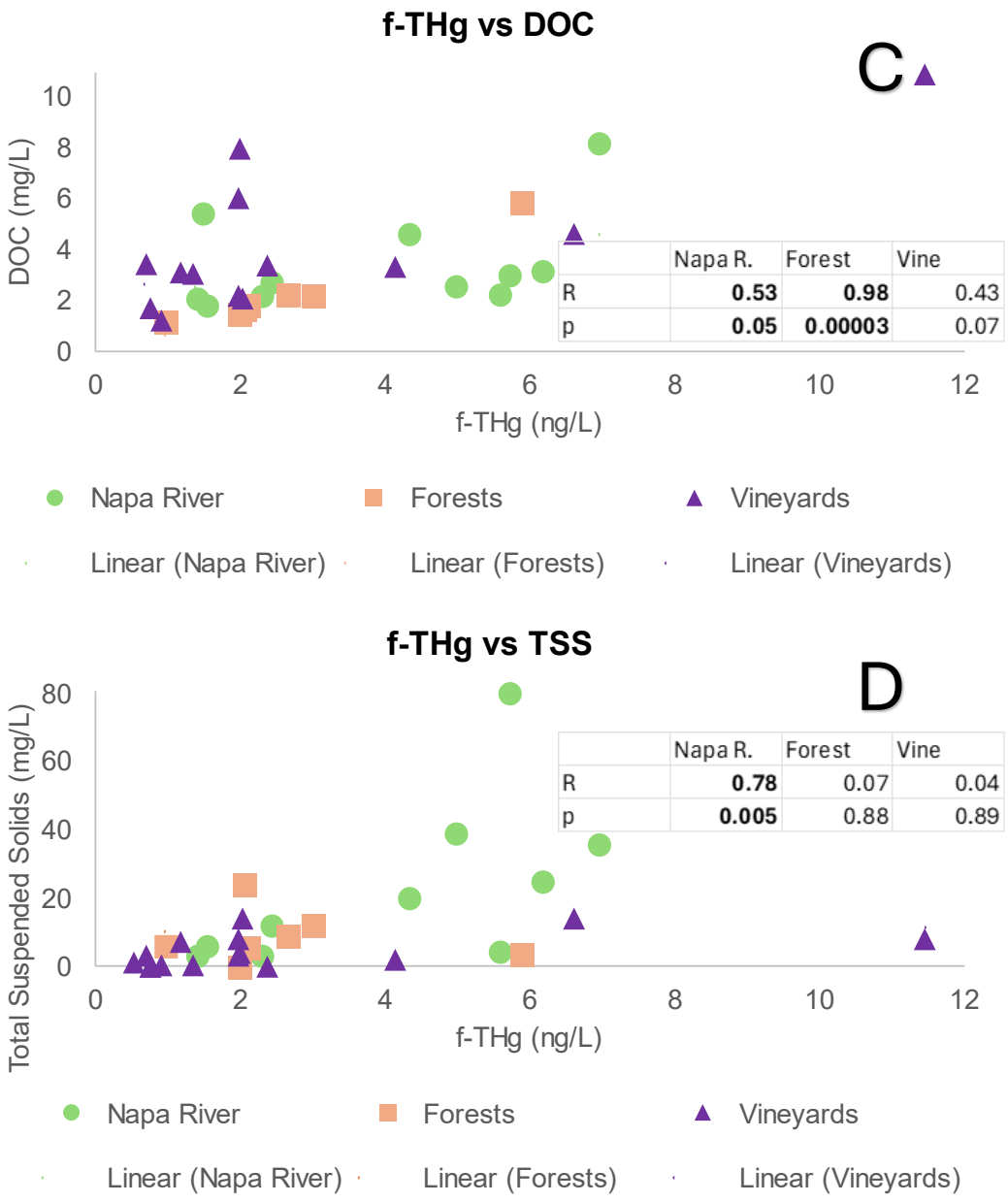

Figure 16. Correlation plots showing the relationships between (A) fitered-THg and filtered-MeHg, (B) filtered-THg and SO_4^{2-}, (C) filtered-THg and DOC, and (D) filtered-THg and TSS. Linear regressions performed on each data subset and Spearman's rank correlation coefficient "R" reported with associated p-value. Statistically significant associations are bolded in data table.

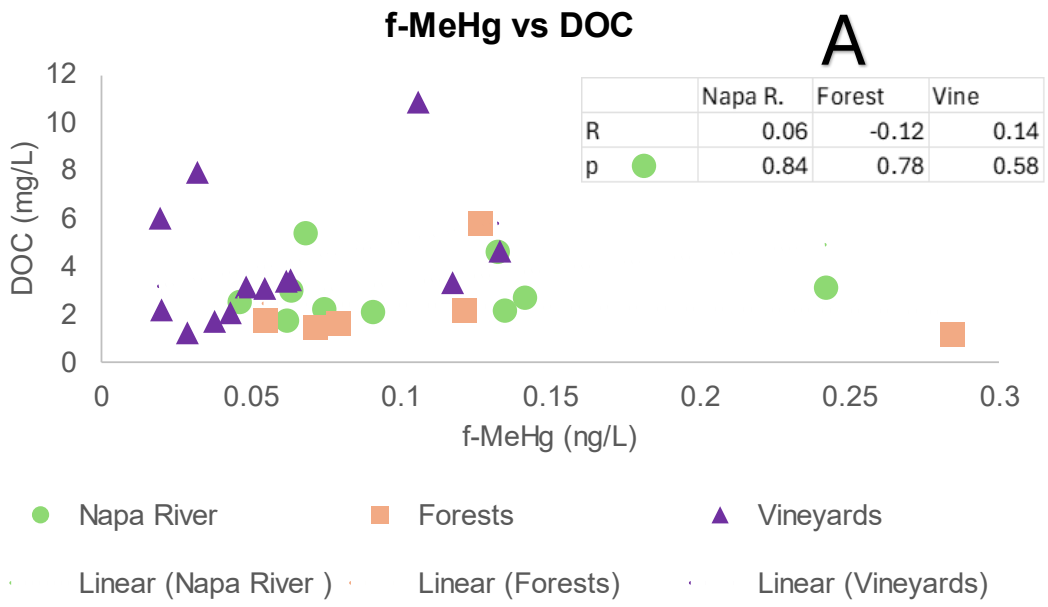
f-MeHg vs DOC
A
DOC (mg/L)
f-MeHg (ng/L)
Napa R. Forest Vine
R 0.06 -0.12 0.14
p 0.84 0.78 0.58
Napa River
Forests
Vineyards
Linear (Napa River)
Linear (Forests)
Linear (Vineyards)

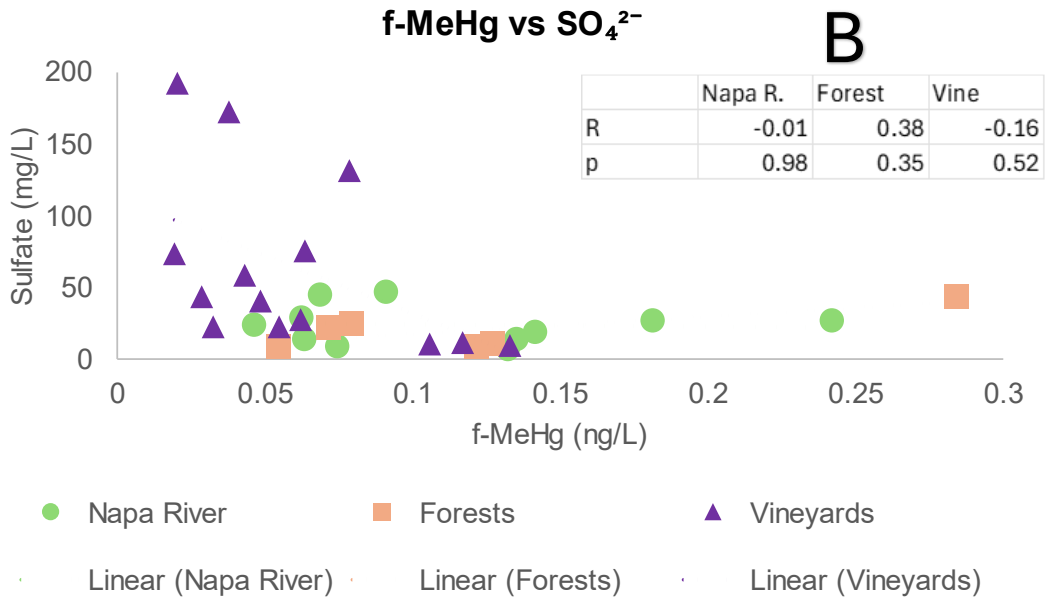
f-MeHg vs SO_4^{2-}
B
Sulfate (mg/L)
f-MeHg (ng/L)
Napa R. Forest Vine
R -0.01 0.38 -0.16
p 0.98 0.35 0.52
Napa River
Forests
Vineyards
Linear (Napa River)
Linear (Forests)
Linear (Vineyards)

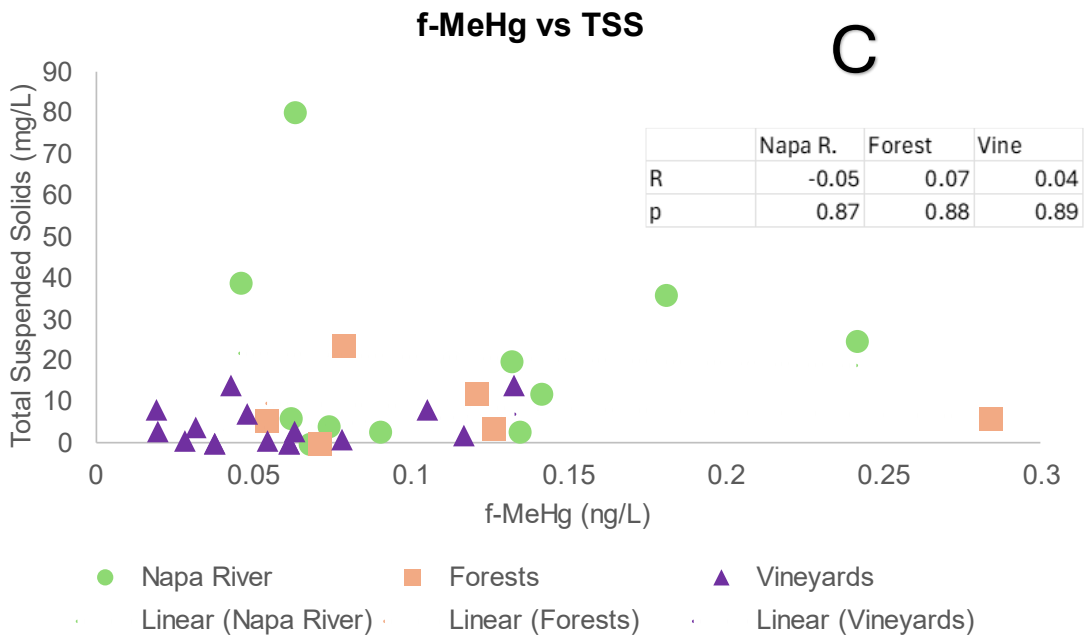

Figure 17. Correlation plots showing the relationships between (A) filtered-MeHg and DOC, (B) filtered-MeHg and SO_4^{2-}, and (C) filtered-MeHg and TSS. Linear regressions performed on each data subset and Spearman's rank correlation coefficient "R" reported with associated p-value. Statistically significant associations are bolded in data tables.

particulate fraction, whereas f-THg is in the dissolved fraction which removes many of the substrates to which Hg adsorbs.

In Figure 17 correlation plots, there is a general lack of correlations amongst f-MeHg and ancillary analytes. The only relationship that explained any variability in f-MeHg was with SO_4^{2-} in the background forest samples at almost 56%. Vineyard samples show a negative correlation between f-MeHg/SO_4^{2-} which is what was observed in the f-THg/SO_4^{2-} relationship as well. This leads to the hypothesis that complex formation may be sequestering Hg making it less bioavailable, and attenuating MeHg abundance. Furthermore, this is more data pointing to agricultural S inputs influencing Hg's fate. Figure 17C shows the relationships between f-MeHg and TSS which were not correlated at all. This is potentially illuminating the difference between what is observed in the dissolved versus particulate fraction.

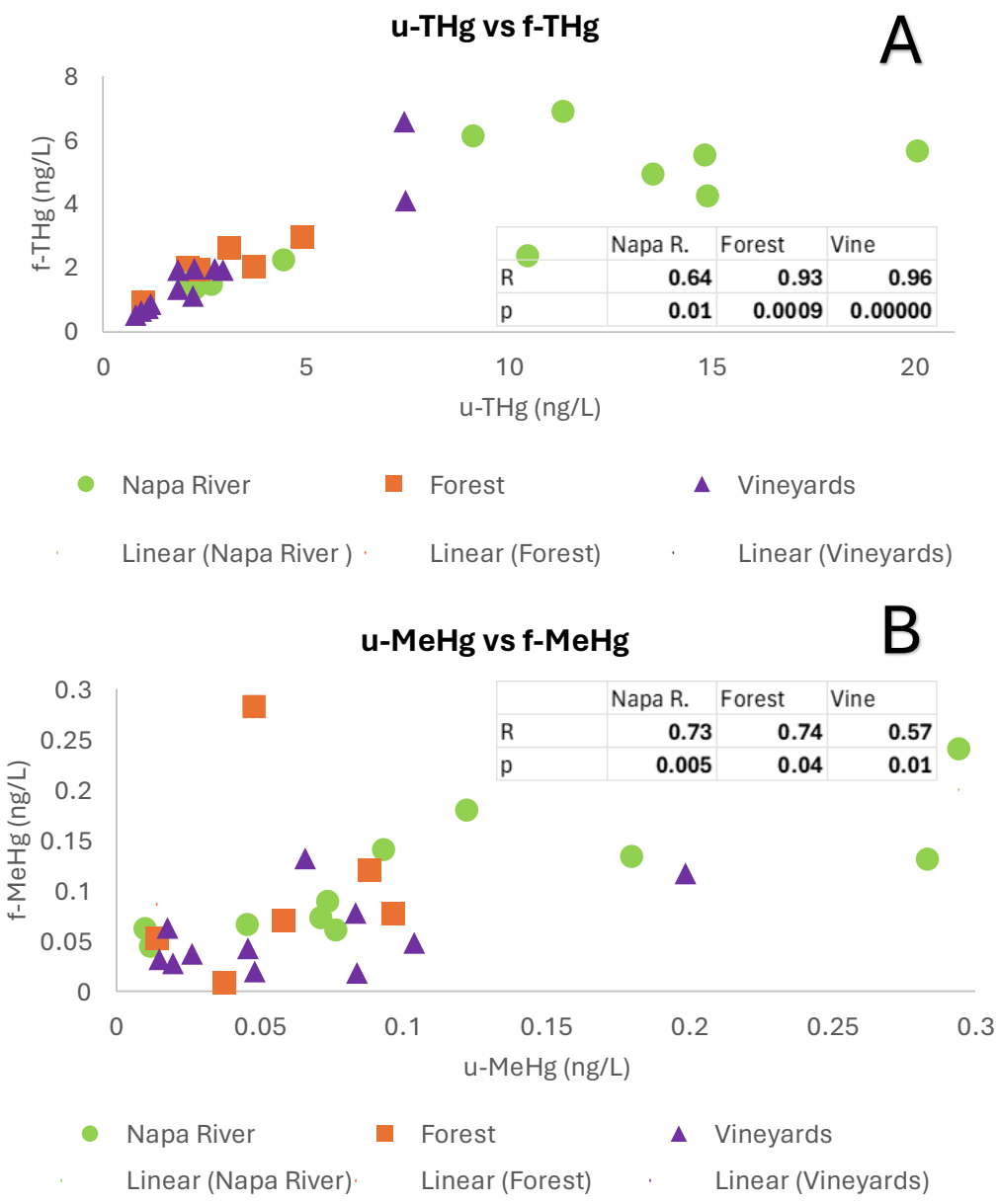

Figure 18. Correlation plots showing the relationships between (A) unfiltered-THg and filtered-THg, and (B) unfiltered-MeHg and filtered-MeHg. Linear regressions performed on each data subset and Spearman's rank correlation coefficient "R" reported with associated p-value. Statistically significant associations are bolded in data table.

The correlation plots in Figure 18 show the relationships between dissolved and particulate fractions of (A) THg and (B) MeHg. All correlations were determined to be positively correlated and statistically significant with the highest being identified in THg in the vineyard

samples with an R-value of 0.96. The values for THg were more highly correlated for vineyard (0.96) and forest (0.93) samples, whereas the NR (0.64) samples were not as strongly correlated but still significant. Interestingly, for MeHg, the forest (0.74) and NR (0.73) samples had stronger correlations and the vineyards (0.57) were not as strongly correlated but still significant.

3.4 Paired Sites. Vineyard sites were paired with background sites to compare the difference between samples with and without agricultural influence. Paired sites in this study include CFB with CVE, and TFB with HVD, PVD, and PVE. The results of the vineyards were tested against the results of the background sites. Figure 4 is an aerial map view of the entire study area showing the geographic relationship between test sites and background sites. Additionally, site position within the watershed is seen and location relative to the Napa River. In Figure 5, site CFB's high position in the watershed illustrates its lack of potential anthropogenic influence regarding agrarian practices and legacy mining operations. Figure 6 shows the geographic relationship between background forest (TFB) and vineyard test sites (HVD, PVD, PVE). TFB's position is proximal to the toe of forested lands approaching the valley floor. The overlying land cover above this site position in the watershed is mountainous undeveloped forest.

3.4.1 CFB vs CVE. For u-THg at CVE there is an apparent elevation in the measured values at the test site versus background values (Figure 19 and 21). An agricultural signal was evident as there was an impact on MeHg abundance. The difference was statistically analyzed with a T-Test and subsequent F-Test (Table 2) which resulted in significantly different means ($p<0.05$). Regarding u-MeHg, the vineyard test site (CVE) also showed an agricultural influence as compared to the background site (CFB). The averaged values of u-MeHg were higher than the averaged values obtained at the background site but resulted in no significant difference between means ($p<0.05$). It should also be stated that even though it

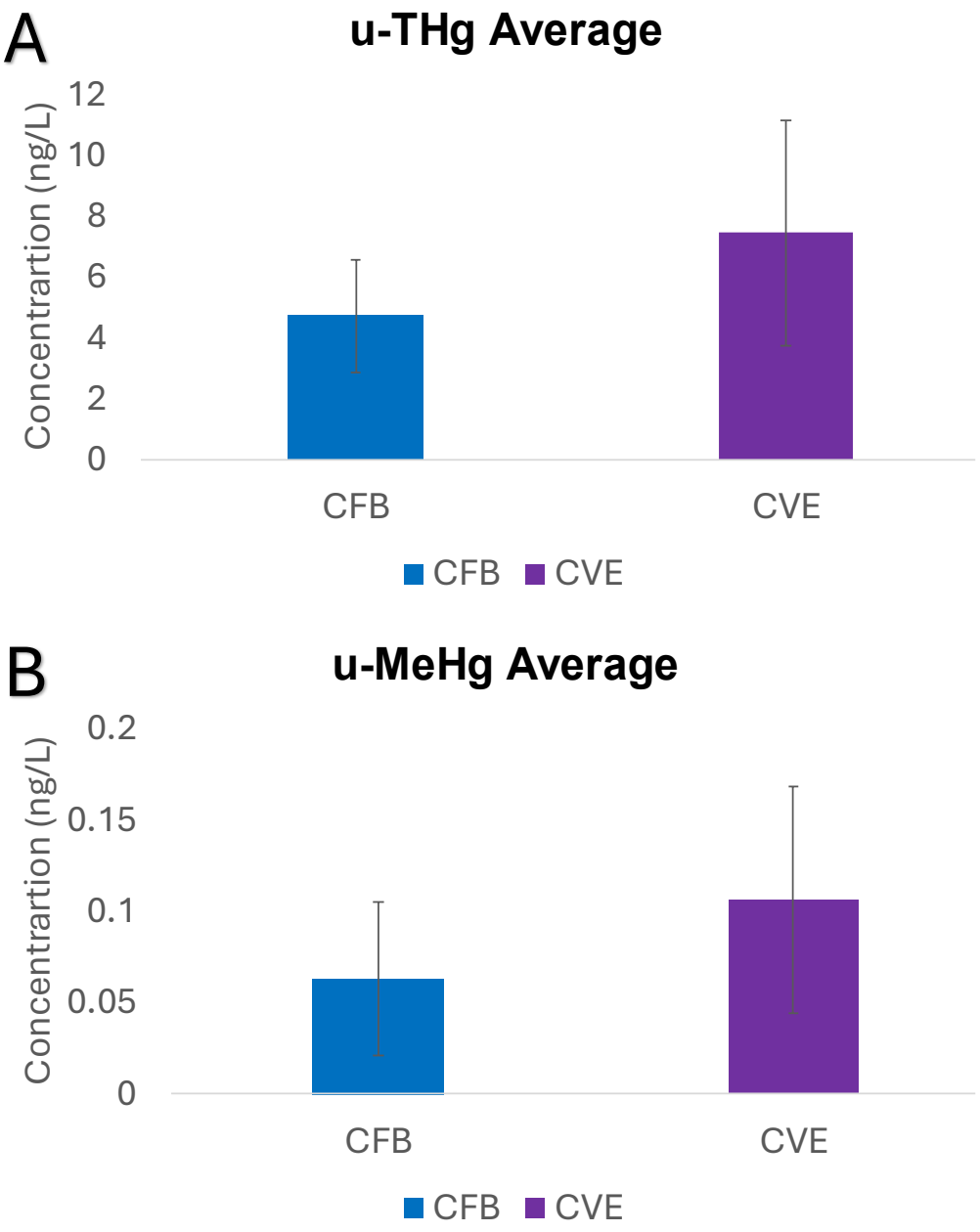

Figure 19. Paired sites CFB (vineyard C, forest background) and CVE (vineyard C, vineyard effluent) are shown comparing the averages of (A) unfiltered-THg (ng/L) and (B) unfiltered-MeHg (ng/L). For site CFB, n=3; for site CVE, n=4. Error bars indicate the relative standard deviation.

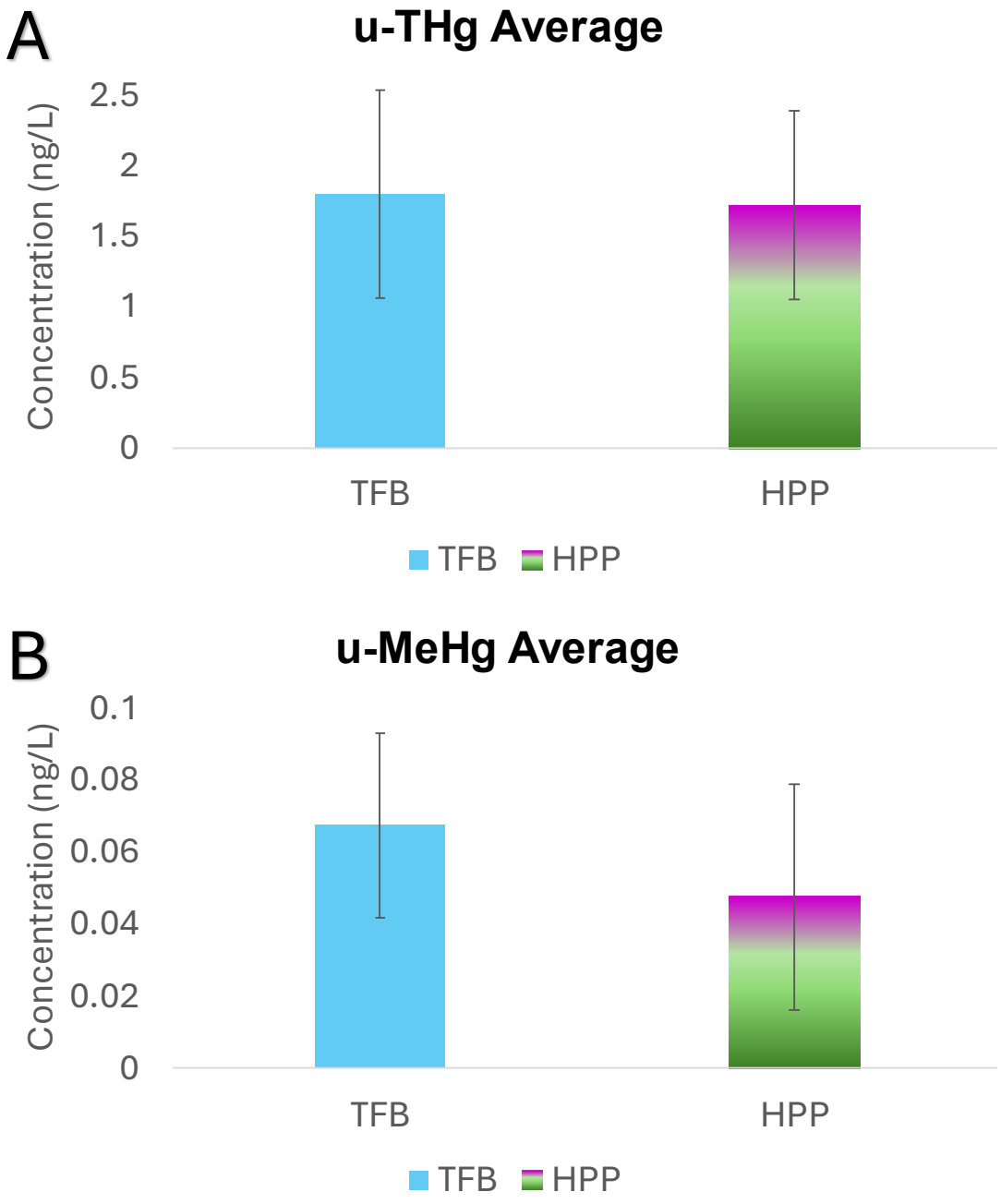

Figure 20. Paired sites TFB (vineyard T, forest background) and HPP aggregate (HVD, PVD, PVE (vineyard sites H-ditch, P-ditch, and P-effluent)) are shown comparing unfiltered-THg and unfiltered-MeHg averages (ng/L). For site TFB, n=3; for aggregate site HPP, n=10. Error bars indicate the relative standard deviation.

appeared higher than background values, the values hovered around the “pristine” water threshold ($\leqslant$ 0.10 ng/L) and below (Rudd, 1995).

Ancillary analyte comparisons were also analyzed between vineyards and forested background sites. CFB vs CVE data showed excess abundance in DOC and SO_4^{2-} at the test site (Figure 21). Average DOC and SO_4^{2-} values, 6.22 mg/L and 26.58 mg/L respectively, were both nearly double the background DOC and SO_4^{2-} average values of 3.03 mg/L and 12.29 mg/L, respectively. However, despite the agricultural signal identified in the vineyard samples, the means were not statistically different ($p<0.05$). TSS values were essentially the same between test and background sites. This contrasts trends observed by other mercury researchers who have correlated higher MeHg/THg concentrations with higher loads of suspended solids.

3.4.2 TFB vs HPP. Forested background site TFB u-THg averages were compared to the paired site HPP (Figure 20), an aggregate of HVD, PVD, and PVE sites, u-THg averages. As seen in Figure 20, test site sample averages were not higher than the background sites illustrating the lack of agricultural signal. The results of u-MeHg comparison also showed a lack of agricultural signal as the test sites were lower in u-MeHg abundance.

The average concentration of DOC was 2X higher at the vineyard test site (3.15 mg/L) versus forested background (1.44 mg/L) but did not have statistically different means ($p<0.05$). The results of the SO_4^{2-} comparison between test sites HPP and background site TFB showed the clearest agricultural signal of the entire study (Figure 21). HPP average SO_4^{2-} value (78.80 mg/L) was more than 2X as much as TFB's average SO_4^{2-} value (31.01 mg/L). Statistical analysis (T-Test and F-Test) determined that TFB and HPP SO_4^{2-} means were significantly different ($p<0.05$) with an F-Test score of 0.03. The results of the SO_4^{2-} data show agricultural inputs are significant and speak to the geographic position of HPP sites in the watershed as they are the most influenced by agriculture practices involving SO_4^{2-}

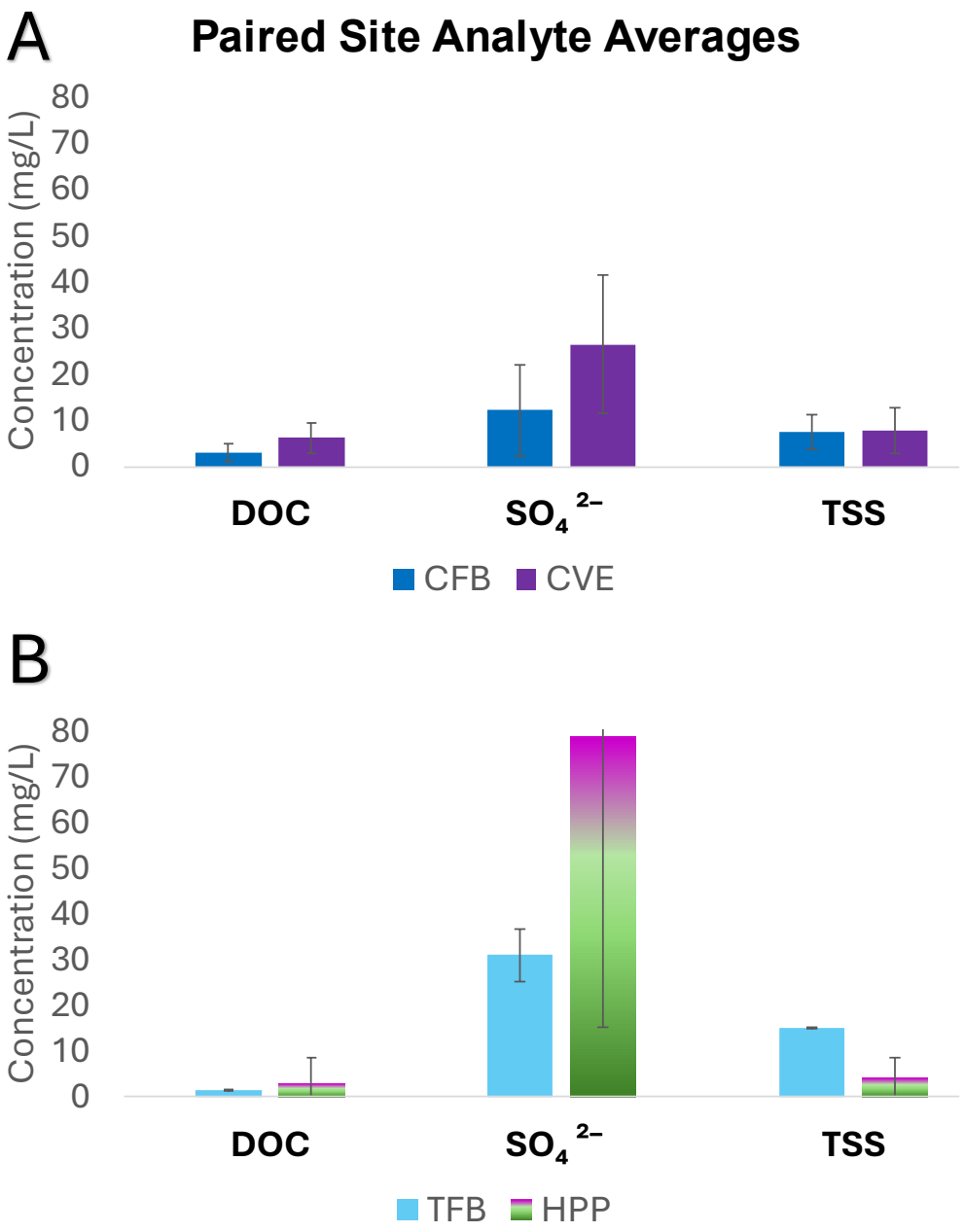

Figure 21. Averaged ancillary analyte concentrations of SO_4^{2-}, DOC, and TSS for vineyards and their paired forested background sites shown in units of milligrams per liter (mg/L). Paired sites (A) CFB (vineyard C, forest background) with CVE (vineyard C, effluent) are compared against each other, as well as (B) TFB (vineyard T, forest background) and HPP aggregate (vineyard sites H-ditch, P-ditch, and P-effluent). For site CFB, n=3; for site CVE, n=4. For site TFB, n=3; for aggregate site HPP, n=10. Error bars indicate the relative standard deviation.

amendments and fungicide application. Therefore, we see that high SO_4^{2-} abundance may be a factor in the Hg species immobilization, via Hg-complex formation (Frohne et al., 2012; Manceau et al., 2015), resulting in low THg and MeHg concentrations measured in fluvial waters at these vineyard sites. TSS data was inconclusive with a higher background site average versus vineyard sites.

4. Discussion

4.1 Hydrogeology. Episodic precipitation events control the fluvial discharge volumes in the Napa River and its tributaries. The structure of the watershed is linear-to-narrow and is bound by mountain ranges on both sides of the valley floor with rapid drainage which dictates the rising and falling limbs of the hydrograph. As such, there is little time between precipitation events and the rise and fall of the limbs of the hydrograph. This factor has a significant influence on proper sample acquisition timing. Efforts to collect *first flush* data at the beginning of the 2022-2023 rainy season were thwarted due to record precipitation events that persisted for over a month. Conditions were not conducive to sample acquisition as it is not feasible during active precipitation. The opportunity to collect *first flush* data presented itself in December 2023, as the beginning of the 2023-2024 rainy season had a significant initial precipitation event. However, little hydrologic resistance coinciding with rapid drainage characteristics of the NRW resulted in collection of only 3 samples. The groundwater supply had yet to rise to wet season baseflow conditions enabling full hydrologic connectivity. CFB, CVE, and HVD were the only sites where flow was sufficient to collect a proper sample.

Concentrations for all analytes (Figure 12, 13, 14, and 15), except SO_4^{2-}, were highest during periods of elevated fluvial discharge volume following large precipitation events after wet season baseflow conditions were present. The correlation with higher discharge volume and higher analyte concentrations is consistent with trends other Hg researchers have identified (Conaway et al., 2002; Balogh et al., 2002; Kolipinski et al., 2020). We expected to see

elevated MeHg concentrations in irrigation waters draining vineyards given the measured SO_4^{2-} abundance in the watershed, but the concentrations observed were far below what would be considered MeHg pollution.

4.2 Fluvial MeHg Characterization. Surprisingly, no federally mandated water quality standards exist regarding methylmercury in drinking or surface waters. The following information is provided as a reference for what “pristine” to polluted MeHg levels would look like; waterways and bodies of water are unofficially classified as “pristine” if MeHg concentrations are $\leqslant$ 0.10 ng/L (Rudd, 1995). Fluvial systems considered *potentially* negatively impacted have MeHg concentrations above 0.10 ng/L (Domagalski 2001; Rudd, 1995). In a report sent to the U.S. EPA by the California Regional Water Quality Control Board in 2000, they proposed “A dissolved methylmercury target in water of 0.1 ng/L protects human health, based on the FDA action level of 1 mg/kg in fish tissue and a bioaccumulation factor of 10 million”. This derivation was based on substituting the FDA action level of 1 mg/kg for [MeHg] in fish and a bioaccumulation factor of 10^7 yielding a target of 0.1 ng/L MeHg in water. They claim, “this is the concentration limit for methylmercury in water that will keep mercury concentrations in fish at or below 1 mg/kg”. In addition to the aforementioned target already in place, they have proposed a more protective target (0.05 ng/L) based on species specific bioaccumulation factors to protect both wildlife and human subsistence fishers in the San Francisco Bay (CA Regional Water Quality Control Board, 2000). The U.S. Geological Survey conducted a pilot study (Krabbenhoft et al., 1999) to ascertain MeHg concentrations in ambient surface water on a national scale. From 106 sites consisting of 21 basins, they quantified a mean background level of 0.13 ng/L and a mean concentration for all sites of 0.15 ng/L. Fluvial systems considered to have elevated MeHg concentrations are on the order of 1.3 ng/ L, as observed by Balogh et al., 2002 in a predominantly agricultural watershed. Balogh et al. also observed extremely elevated MeHg concentrations (0.44 to 4.90 ng/L) in the Little Cobb River, a third-order stream draining the Le Sueur River

Watershed in the Minnesota River Basin. These reported levels seen by Balogh et al. were cases of elevated and extreme MeHg concentrations characterized as polluted waters. The sources of elevated and extreme [MeHg] resulted from algal blooms and litterfall/throughfall, respectively.

The majority of vineyard/forested background MeHg results fell into the category of “pristine” water. The total number of samples that exceeded the 0.10 (ng/L) threshold was 16, of this, 9 were from the Napa River and 7 from vineyards/forested background sites. Only 19% of all MeHg results in the study were characterized as *potentially* negatively impacted. Measurements exceeding 0.10 ng/L were significantly low, as over 96% of measured samples were quantified below 0.20 ng/L, and all quantified values were below 0.3 ng/L. The MeHg concentrations observed in this study were not at actionable levels. These are essentially “good” results for farmers, fish, and public safety given the current regulatory criterion.

4.3 Mercury Mobility Factors. A possible explanation for low MeHg concentrations may be the influence of a phenomenon identified by Manceau et al., 2015, where a thermodynamically favorable chemical reaction mechanism in which thiol bound mercury polymerizes forming mercury−sulfur clusters. Cluster formation is driven by elimination of sulfur from the thiol complexes by mercury−sulfur bonds breaking, similar to an alkylation reaction, but without the requisite addition of sulfide. Hg immobilization and eventual sequestration may result from this nucleation mechanism in oxygenated surface environments (Manceau et al., 2015). Another chemical factor linking Hg and S is HgS formation under reducing conditions (Frohne et al., 2012). Available Hg is less abundant and MeHg production rates are lower. Furthermore, limited MeHg production has been observed when Hg is sequestered in a crystalline complex with sulfides or thiol group bound in macromolecular natural organic matter (Manceau et al., 2015). Lower MeHg production rates or reduced mobility result in lower aqueous MeHg abundance in fluvial waters.

Another geochemical control influencing the fate of Hg is the potential for complexation with DOC. Complexation with DOC would have the opposite effect of the mercury-sulfur clusters phenomenon described above. Hg and MeHg mobility would be enhanced by formation of soluble complexes with DOC (Frohne et al., 2012), and would likely result in higher abundance of aqueous Hg species. Understanding Hg and DOC bond formation is a fundamental component to predict Hg speciation and fate in natural environments. Hg-DOC complex strength is strongly influenced by DOC aromaticity wherein the bond strength increases with increased molecular weight and DOC aromaticity (Wang et al., 2022). Furthermore, DOC origins are less influential in controlling binding capacities than the specific DOC properties, like aromaticity (Wang et al., 2022).

4.4 Critical Analysis of Analyte Abundance

Mercury. A comparative analysis of Hg concentrations measured in northern California shows the similarity in values obtained by other Hg researchers and those quantified within this study (Table 2).

THg. The concentrations of THg (Figure 12 and 13) in this study were slightly elevated compared to what other researchers have seen in fluvial waters in temperate climates (Bravo et al., 2018). However, none of the quantified values exceeded the current and state and federal recommended criterion for protection of aquatic life which is set at 1400 ng/L for acute exposure and 770 ng/L for chronic exposure. To give context to the difference in order of magnitude between the quantified values seen in this study and the recommended criterion - the highest THg measurement was 20.09 ng/L which is only 2.6% of the threshold set for chronic exposure criterion which is the lower value of the two. The EPA states on their website that “aquatic life criteria for toxic chemicals are the highest concentration of specific pollutants or parameters in water that are not expected to pose a significant risk to the majority of species in a given environment or a narrative description of the desired conditions

Location	THg (ng/L)		MeHg (ng/L)		%MeHg	Reference
	Unfiltered	Filtered	Unfiltered	Filtered		
Napa River 1	(4.34 - 14.90) $\bar{x}$ = 11.36	(2.28 - 5.58) $\bar{x}$ = 4.05	(.072 - .28) $\bar{x}$ = .18	(.074 - .14) $\bar{x}$ = .11	u=1.57% f=2.80%	This study, Napa River Watershed
Napa River 2	(2.67 - 20.09) $\bar{x}$ = 11.07	(1.52 - 5.72) $\bar{x}$ = 3.23	(.076 - .093) $\bar{x}$ = .085	(.062 - .14) $\bar{x}$ = .087	u=0.77% f=2.76%	
Napa River 3	(2.05 - 13.57) $\bar{x}$ = 8.30	(1.39 - 6.56) $\bar{x}$ = 4.24	(.012 - .29) $\bar{x}$ = .12	(.046 - .24) $\bar{x}$ = .13	u=1.44% f=3.02%	
Napa River 4	(2.27 - 11.3) $\bar{x}$ = 6.80	(1.39 - 6.95) $\bar{x}$ = 4.17	(.074 - .12) $\bar{x}$ = .098	(.090 - .18) $\bar{x}$ = .14	u=1.44% f=3.26%	
South Fork Eel River	(0.71 - 1.21)	(0.56 - 0.88)	(.13 - .17)	(.04 - .12)	u= 18.3-14.1% f=7.14-13.6%	Tsui et al., 2009, Hg Bioaccumulation, N. California
Elder 1	(0.40 - 0.95)	(0.35 - 0.57)	(.03 - .04)	(.03 - .04)	u= 7.5-4.21% f= 7.02-8.57%	
Sac River at Colusa	(2.0 - 105) median=		(.06 - .43)		u= 0.41%	Domagalski 2001, Sacramento

	43.5		$\bar{x}$ = .10			River and Tributaries
Sac Slough, Knights Landing	(5.0 - 16.0)		(.07 - .57) median= .15		u= 1.4-3.56%	
Colusa Basin Drain, Knight Landing	(5.0 - 14.0)		(.08 - .38) median= .19		u= 1.6-2.7%	
Sac River at Freeport	(2.0 - 13.0)		(.03 - .29) median= .12		u= 1.5-2.23%	
Sac River at Verona	(3.0 - 18.0)		(.05 - .42) median= .13		u= 1.67-2.33%	
Sacramento River Watershed			(0.02 - 1.98) LSmean = 0.18			Tanner, et. al. 2017, The Contribution of Rice Ag to MeHg
29 european streams	(0.06 - 2.78)		(0.007 - 0.16)		u= 11.7 - 5.76%	Bravo et al., 2018, The Interplay

Table 2. This table shows Hg concentrations from this study and other studies in the northern California region (LSmean = Least Squares mean). The region in which these studies were performed contain many legacy mining operations that contributed to the total Hg abundance currently present in sediments and bodies of water in parts of northern California.

of a water body being "free from" certain negative conditions". It must also be stated that the

EPA is working to revise its current water quality criteria for Hg. They have released the

following statement “It is important to note that the mercury aquatic life criterion includes a caution that it might not be adequately protective of such important fishes as the rainbow trout, coho salmon and bluegill. The criterion was derived from inorganic mercury (II) data but is applied to total mercury and may be under-protective if a substantial portion of the mercury in the water column is methylmercury. Also, even though inorganic mercury is converted to methylmercury and methylmercury bioaccumulates to a great extent, this criterion does not account for uptake via the food chain because sufficient data were not available when the criterion was derived”. Considering these issues, the EPA is working on an update to the mercury criterion.

5. Conclusions

5.1 Mercury and Hg/DOC Entanglement. Overall, the study results elucidated acceptable MeHg species abundance in NRW fluvial waters. The paired sites CFB and CVE revealed higher MeHg concentrations in the vineyard than in the background suggesting that agricultural processes had an impact. Despite the noted impact, MeHg concentrations were still relatively low and action levels (action levels are only suggestions, no legislative controls currently exist in NRW) were not reached. Given the concentrations of THg it was expected that the data would show higher concentrations of MeHg as the ingredients needed for methylation (THg, DOC, and SO_4^{2-}) were present. THg concentrations were well below EPA maximum contaminant levels (2000 ng/L) for drinking water. However, THg measurements in this study were slightly elevated compared to what other researchers (Bravo et al., 2018) have identified as typical fluvial concentrations for an aquatic system without any geologic or anthropogenic point sources (<0.05 to 12 ng/L) (Dennis et al., 2005; Driscoll et al., 2007; Wiener et al., 2003). With known geologic mercury deposits in this geologic province, we expected to see higher fluvial THg concentrations. Relationships between DOC and THg were strongly impacted by filtration as no positive correlations were made between DOC and THg in undissolved fractions. However, there was no difference for MeHg abundance in the

dissolved or particulate fractions which highlights the importance of the dissolved fraction and its influence on the affinity of Hg with DOC and for the diverging processes controlling the two Hg species abundance (Lavoie et al., 2022). Positive correlations between DOC and THg in this study were identified in the dissolved fraction at vineyard sites with the highest correlation found within forested background sites.

5.2 Trending SO_4^{2-}. A salient agricultural signal of high SO_4^{2-} abundance was identified in vineyard locations. Compared to other recent studies (Hermes et al., 2022), average SO_4^{2-} abundance was 2 - 8x higher depending on position in the watershed. The highest vineyard values were identified at locations that were the furthest downgradient and thus subject to the most anthropogenic influence. While high SO_4^{2-} abundance is proposed to enhance MeHg production via SRB stimulation, no elevated MeHg concentrations were observed in the study. Sites identified with the highest SO_4^{2-} values also had the lowest methylation rates in a parallel study (Weiss et al., unpublished). The expectation going into the study was to observe the opposite trend in MeHg generation. HgS formation, and other complex formations, may potentially be impacting Hg mobility resulting in low measured aqueous concentrations. The only statistically significant comparisons were observed between the paired sites TFB and HPP regarding SO_4^{2-} and DOC. The SO_4^{2-} abundance in the vineyards (HPP) was over 2x the average abundance at TFB. Paired sites CFB & CVE were shown to have the least agricultural SO_4^{2-} loading impact, undoubtedly due to their high placement in the watershed. That said, intra-vineyard SO_4^{2-} loading was evident at CVE as evidenced in the data compared to the unimpacted values measured at CFB. A notable trend was observed progressing downstream in the Napa River as [SO_4^{2-}] revealed an increasing pattern present in all (3) sample sets. This result is clearly driven by the agrarian landscape practices of fungicidal sulfur applications. The SO_4^{2-} measurements made in this study were relatively high, 2 - 8x higher depending on watershed position, when compared to other researchers' findings in the NRW (Hermes et al., 2022). By far, the site that had the highest

[SO_4^{2-}] was PVE. Unsurprisingly, this vineyard site was furthest downgradient within the watershed, in this study.

5.3 Synopsis. To sum up the big picture, the results are good for farmers, fish, and public safety given current regulatory parameters. The main concern prompting investigation into agricultural practices impacting MeHg levels in NRW fluvial waters has been at least partially answered. We did not see any proof in the data that sulfur fungicide applications positively influenced higher MeHg production rates resulting in elevated fluvial MeHg concentrations. Furthermore, there were no point sources of pollution identified in this study as there were no instances of elevated MeHg concentrations identified. Further research is needed to resolve mercury mobility, suppressed MeHg production in high sulfate environments, and geochemical controls on Hg abundance and speciation in fluvial systems.

References

Alpert, A., E. Czaika, and A. Giang, “Mercury’s Health Effects,” Mercury Science and Policy, 2013.

Balogh, Steven J., Yabing Huang, Heather J. Offerman, Michael L. Meyer, and D. Kent Johnson. “Episodes of Elevated Methylmercury Concentrations in Prairie Streams.” *Environmental Science & Technology* 36, no. 8 (April 1, 2002): 1665–70. https://doi.org/10.1021/es011265w.

Barkay, Tamar, and Irene Wagner-Döbler. “Microbial Transformations of Mercury: Potentials, Challenges, and Achievements in Controlling Mercury Toxicity in the Environment.” In *Advances in Applied Microbiology*, 57:1–52. Academic Press, 2005. https://doi.org/10.1016/S0065-2164(05)57001-1.

Bloom, N.S., Von Der Geest, E.J. Matrix modification to improve the recovery of MMHg from clear water using distillation. *Water Air Soil Pollut* **80**, 1319–1323 (1995). https://doi.org/10.1007/BF01189797

Bloom, N. S. Can. J. Fish. Aquat. Sci. 1992, 49, 1010-1017

Bloom, N. S., and C. J. Watras. “Observations of Methylmercury in Precipitation.” *Science of The Total Environment*, Trace Metals in Lakes, 87–88 (November 1, 1989): 199–207. https://doi.org/10.1016/0048-9697(89)90235-0.

Bloom, Nicolas S., and Eric A. Crecelius. “Determination of Mercury in Seawater at Sub-Nanogram per Liter Levels.” *Marine Chemistry* 14, no. 1 (November 1, 1983): 49–59. https://doi.org/10.1016/0304-4203(83)90069-5.

Bloom, Nicolas, and William F. Fitzgerald. “Determination of Volatile Mercury Species at the Picogram Level by Low-Temperature Gas Chromatography with Cold-Vapour Atomic Fluorescence Detection.” *Analytica Chimica Acta* 208 (1988): 151–61. https://doi.org/10.1016/S0003-2670(00)80743-6.

Bravo, Andrea G., and Claudia Cosio. “Biotic Formation of Methylmercury: A Bio–Physico–Chemical Conundrum.” *Limnology and Oceanography* 65, no. 5 (May 1, 2020): 1010–27. https://doi.org/10.1002/lno.11366.

Bravo, Andrea G., Dolly N. Kothawala, Katrin Attermeyer, Emmanuel Tessier, Pascal Bodmer, José L. J. Ledesma, Joachim Audet, et al. “The Interplay between Total Mercury, Methylmercury and Dissolved Organic Matter in Fluvial Systems: A Latitudinal Study across Europe.” *Water Research* 144 (November 1, 2018): 172–82. https://doi.org/10.1016/j.watres.2018.06.064.

Bravo, Andrea G., Dolly N. Kothawala, Katrin Attermeyer, Emmanuel Tessier, Pascal Bodmer, and David Amouroux. “Cleaning and Sampling Protocol for Analysis of Mercury and Dissolved Organic Matter in Freshwater Systems.” *MethodsX* 5 (2018): 1017–26. https://doi.org/10.1016/j.mex.2018.08.002.

California Regional Water Quality Control Board San Francisco Bay Region “Watershed Management of Mercury in the San Francisco Bay Estuary: Total Maximum Daily Load Report to U.S. EPA.”

https://www.waterboards.ca.gov/sanfranciscobay/water_issues/available_documents/aug00hgtmdl.pdf, June 30, 2000. Date accessed 5/15/2024. Principal authors and editors: Dr. Khalil E. Abu-Saba and Lila W. Tang, PE.

California Waterboards State Water Resources Control Board "San Francisco Bay Mercury TMDL." www.waterboards.ca.gov/water_issues/programs/mercury/other_programs.html#fishadv, Updated 6/27/18. Date accessed 5/10/2024.

Compeau, G. C., and R. Bartha. "Sulfate-Reducing Bacteria: Principal Methylators of Mercury in Anoxic Estuarine Sediment." *Applied and Environmental Microbiology* 50, no. 2 (August 1985): 498–502. https://doi.org/10.1128/aem.50.2.498-502.1985.

Cooper, Connor J., Kaiyuan Zheng, Katherine W. Rush, Alexander Johs, Brian C. Sanders, Georgios A. Pavlopoulos, Nikos C. Kyrpides, et al. "Structure Determination of the HgcAB Complex Using Metagenome Sequence Data: Insights into Microbial Mercury Methylation." *Communications Biology* 3, no. 1 (June 19, 2020): 1–9. https://doi.org/10.1038/s42003-020-1047-5.

Dennis, Ian F., Thomas A. Clair, Charles T. Driscoll, Neil Kamman, Ann Chalmers, Jamie Shanley, Stephen A. Norton, and Steve Kahl. "Distribution Patterns of Mercury in Lakes and Rivers of Northeastern North America." *Ecotoxicology* 14, no. 1 (March 1, 2005): 113–23. https://doi.org/10.1007/s10646-004-6263-0.

Domagalski, Joseph. "Mercury and Methylmercury in Water and Sediment of the Sacramento River Basin, California." *Applied Geochemistry* 16, no. 15 (December 1, 2001): 1677–91. https://doi.org/10.1016/S0883-2927(01)00068-3.

Driscoll, Charles T, Kimberley M Driscoll, Myron J Mitchell, and Dudley J Raynal. "Effects of Acidic Deposition on Forest and Aquatic Ecosystems in New York State." *Environmental Pollution*, Environmental Monitoring, Evaluation and Protection in New York: Linking Science and Policy, 123, no. 3 (June 1, 2003): 327–36. https://doi.org/10.1016/S0269-7491(03)00019-8.

Driscoll, Charles T., Young-Ji Han, Celia Y. Chen, David C. Evers, Kathleen Fallon Lambert, Thomas M. Holsen, Neil C. Kamman, and Ronald K. Munson. "Mercury Contamination in Forest and Freshwater Ecosystems in the Northeastern United States." *BioScience* 57, no. 1 (January 1, 2007): 17–28. https://doi.org/10.1641/B570106.

Fisher, L. Suzanne, and Mark H. Wolfe. "Examination of Mercury Inputs by Throughfall and Litterfall in the Great Smoky Mountains National Park." *Atmospheric Environment* 47 (February 1, 2012): 554–59. https://doi.org/10.1016/j.atmosenv.2011.10.017.

Frohne, T., J. Rinklebe, U. Langer, G. Du Laing, S. Mothes, and R. Wennrich. "Biogeochemical Factors Affecting Mercury Methylation Rate in Two Contaminated Floodplain Soils." *Biogeosciences* 9, no. 1 (January 26, 2012): 493–507. https://doi.org/10.5194/bg-9-493-2012.

Gilmour, Cynthia C., Dwayne A. Elias, Amy M. Kucken, Steven D. Brown, Anthony V. Palumbo, Christopher W. Schadt, and Judy D. Wall. "Sulfate-Reducing Bacterium Desulfovibrio Desulfuricans ND132 as a Model for Understanding Bacterial Mercury

Methylation." *Applied and Environmental Microbiology* 77, no. 12 (June 15, 2011): 3938–51. https://doi.org/10.1128/AEM.02993-10.

Graymer, R.W., E.E. Brabb, D.L. Jones, J. Barnes, R.S. Nicholson, and R.E. Stamski.Geologic Map and Map Database of Eastern Sonoma and Western Napa Counties, California. 2007. U.S. Geological Survey Scientific Investigations Map 2956. https://pubs.usgs.gov/sim/2007/2956/sim2956i.pdf

Grigal, D F. "Inputs and Outputs of Mercury from Terrestrial Watersheds: A Review." *Environmental Reviews* 10, no. 1 (March 2002): 1–39. https://doi.org/10.1139/a01-013.

Hall, B. D.; Bodaly, R. A.; Fudge, R. J. P.; Rudd, J. W. M.; Rosenberg, D. M. Water, Air, Soil Pollut. 1997, 100,13-24

Hall, B.D., V.L. St. Louis, K.R. Rolfhus, R.A. Bodaly, K.G. Beaty, M.J. Paterson, and K.A. Peech Cherewyk. "Impacts of Reservoir Creation on the Biogeochemical Cycling of Methyl Mercury and Total Mercury in Boreal Upland Forests." *Ecosystems* 8, no. 3 (April 1, 2005): 248–66. https://doi.org/10.1007/s10021-003-0094-3.

Hermes, Anna L., Todd E. Dawson, and Eve-Lyn S. Hinckley. "Sulfur Isotopes Reveal Agricultural Changes to the Modern Sulfur Cycle." *Environmental Research Letters* 17, no. 5 (April 2022): 054032. https://doi.org/10.1088/1748-9326/ac6683.

Hinckley, Eve-Lyn S., and Pamela A. Matson. "Transformations, Transport, and Potential Unintended Consequences of High Sulfur Inputs to Napa Valley Vineyards." *Proceedings of the National Academy of Sciences* 108, no. 34 (August 23, 2011): 14005–10. https://doi.org/10.1073/pnas.1110741108.

Hinckley, Eve-Lyn S., Scott Fendorf, and Pamela Matson. "Short-Term Fates of High Sulfur Inputs in Northern California Vineyard Soils." *Nutrient Cycling in Agroecosystems* 89, no. 1 (January 1, 2011): 135–42. https://doi.org/10.1007/s10705-010-9383-3.

Hinckley, E. S., and P. A. Matson. "Sulfur as a Tracer of Hydrologic and Biogeochemical Dynamics in Northern California Vineyard Soils" 2009 (December 1, 2009): H31I-02.

Hinckley, Eve-Lyn S., John T. Crawford, Habibollah Fakhraei, and Charles T. Driscoll. "A Shift in Sulfur-Cycle Manipulation from Atmospheric Emissions to Agricultural Additions." *Nature Geoscience* 13, no. 9 (September 2020): 597–604. https://doi.org/10.1038/s41561-020-0620-3.

Horvat, Milena, Nicolas S. Bloom, and Lian Liang. "Comparison of Distillation with Other Current Isolation Methods for the Determination of Methyl Mercury Compounds in Low Level Environmental Samples: Part 1. Sediments." *Analytica Chimica Acta* 281, no. 1 (September 1, 1993): 135–52. https://doi.org/10.1016/0003-2670(93)85348-N.

Hsu-Kim, Heileen, Chris S. Eckley, Dario Achá, Xinbin Feng, Cynthia C. Gilmour, Sofi Jonsson, and Carl P. J. Mitchell. "Challenges and Opportunities for Managing Aquatic Mercury Pollution in Altered Landscapes." *Ambio* 47, no. 2 (March 2018): 141–69. https://doi.org/10.1007/s13280-017-1006-7.

Kolipinski, Mietek, Mani Subramanian, Kristina Kristen, Steven Borish, and Stacy Ditta. "Sources and Toxicity of Mercury in the San Francisco Bay Area, Spanning California and

Beyond." *Journal of Environmental and Public Health* 2020 (September 24, 2020): 8184614. https://doi.org/10.1155/2020/8184614.

Krabbenhoft, David P., et al. "A national pilot study of mercury contamination of aquatic ecosystems along multiple gradients." *US geological survey toxic substances hydrology program: proceedings of the technical meeting, Charleston, South Carolina*. Vol. 2. 1999

Kunkel, Fred, and J E Upson. "Geology and Ground Water in Napa and Sonoma Valleys; Napa and Sonoma Counties California," Geological Survey Water-Supply Paper 1495. *California Department of Water Resources*. U.S. Government Printing Office 1960. Pg. 252. N.d.

Lavoie, Raphael A., Marc Amyot, and Jean-François Lapierre. "Global Meta-Analysis on the Relationship Between Mercury and Dissolved Organic Carbon in Freshwater Environments." *Journal of Geophysical Research: Biogeosciences* 124, no. 6 (June 2019): 1508–23. https://doi.org/10.1029/2018JG004896.

Liang, L., M. Horvat, and N. S. Bloom. "An Improved Speciation Method for Mercury by GC/CVAFS after Aqueous Phase Ethylation and Room Temperature Precollection." *Talanta* 41, no. 3 (March 1, 1994): 371–79. https://doi.org/10.1016/0039-9140(94)80141-X.

Luo, Hongwei, Qianqian Cheng, Dongqin He, Jianqiang Sun, Jun Li, and Xiangliang Pan. "Recent Advances in Microbial Mercury Methylation: A Review on Methylation Habitat, Methylator, Mechanism, and Influencing Factor." *Process Safety and Environmental Protection* 170 (February 1, 2023): 286–96. https://doi.org/10.1016/j.psep.2022.12.007.

Lyons, W. Berry, Timothy O. Fitzgibbon, Kathleen A. Welch, and Anne E. Carey. "Mercury Geochemistry of the Scioto River, Ohio: Impact of Agriculture and Urbanization." *Applied Geochemistry*, Mercury: Distribution, Transport, and Geochemical and Microbial Transformations from Natural and Anthropogenic Sources, 21, no. 11 (November 1, 2006): 1880–88. https://doi.org/10.1016/j.apgeochem.2006.08.005.

Manceau, Alain, Cyprien Lemouchi, Mironel Enescu, Anne-Claire Gaillot, Martine Lanson, Valérie Magnin, Pieter Glatzel, et al. "Formation of Mercury Sulfide from Hg(II)–Thiolate Complexes in Natural Organic Matter." *Environmental Science & Technology* 49, no. 16 (August 18, 2015): 9787–96. https://doi.org/10.1021/acs.est.5b02522.

Marvin-DiPasquale, Mark, Lisamarie Windham-Myers, Jennifer L. Agee, Evangelos Kakouros, Le H. Kieu, Jacob A. Fleck, Charles N. Alpers, and Craig A. Stricker. "Methylmercury Production in Sediment from Agricultural and Non-Agricultural Wetlands in the Yolo Bypass, California, USA." *Science of The Total Environment* 484 (June 2014): 288–99. https://doi.org/10.1016/j.scitotenv.2013.09.098.

Method 1630: Methyl Mercury in Water by Distillation, Aqueous Ethylation, Purge and Trap, and Cold Vapor Atomic Fluorescence Spectrometry. August, 1998, 55.

Method 1631, Revision E, August 2002, Final Update to the Mercury in Water by Oxidation, Purge, and Trap, and Cold Vapor Atomic Fluorescence Spectrometry, EPA-821-R-02-019.

Method 160.2, Revision 1999, Total Suspended Solids, Gravimetric. EPA 160.2.CRF.

Napa Watersheds. “Mineral and Rock Resources Napa County Baseline Data Report.” Chapter 2. Version1. www.napawatersheds.org/managed_files/Document/2374/Ch02_MineralResources.pdf, Updated November 30, 2005. Date Accessed 4/5/2024.

Napa Watersheds. Shilling, F., Knapczyk, F., Zlomke, B., Cornwall, C., DiPietro, D., Adams, R., “Technical and Final Report: Application and Findings of the North Bay-Delta Transect Watershed Assessment Framework (WAF)” www.napawatersheds.org/managed_files/Document/4883/20100524_FINAL_w-oAppendicies.pdf May 24, 2010. Date Accessed 5/10/2024.

Neal-Walthall, Natalia, Udonna Ndu, Nelson A. Jr Rivera, Dwayne A. Elias, and Heileen Hsu-Kim. “Utility of Diffusive Gradient in Thin-Film Passive Samplers for Predicting Mercury Methylation Potential and Bioaccumulation in Freshwater Wetlands.” *Environmental Science & Technology* 56, no. 3 (February 1, 2022): 1743–52. https://doi.org/10.1021/acs.est.1c06796.

Obermann, Matthias, Karl-Heinz Rosenwinkel, and Marie-George Tournoud. “Investigation of First Flushes in a Medium-Sized Mediterranean Catchment.” *Journal of Hydrology* 373, no. 3 (July 15, 2009): 405–15. https://doi.org/10.1016/j.jhydrol.2009.04.038.

Parker, Jennifer L., and Nicolas S. Bloom. “Preservation and Storage Techniques for Low-Level Aqueous Mercury Speciation.” *Science of The Total Environment* 337, no. 1–3 (January 2005): 253–63. https://doi.org/10.1016/j.scitotenv.2004.07.006.

Parks, Jerry M., Alexander Johs, Mircea Podar, Romain Bridou, Richard A. Hurt, Steven D. Smith, Stephen J. Tomanicek, et al. “The Genetic Basis for Bacterial Mercury Methylation.” *Science (New York, N.Y.)* 339, no. 6125 (March 15, 2013): 1332–35. https://doi.org/10.1126/science.1230667.

Ranchou-Peyruse, M., M. Monperrus, R. Bridou, R. Duran, D. Amouroux, J. C. Salvado, and R. Guyoneaud. “Overview of Mercury Methylation Capacities among Anaerobic Bacteria Including Representatives of the Sulphate-Reducers: Implications for Environmental Studies.” *Geomicrobiology Journal* 26, no. 1 (January 15, 2009): 1–8. https://doi.org/10.1080/01490450802599227.

Ravichandran, Mahalingam. “Interactions between Mercury and Dissolved Organic Matter—a Review.” *Chemosphere* 55, no. 3 (April 1, 2004): 319–31. https://doi.org/10.1016/j.chemosphere.2003.11.011.

Rogers, R. D. “Methylation of Mercury in Agricultural Soils.” *Journal of Environmental Quality* 5, no. 4 (October 1976): 454–58. https://doi.org/10.2134/jeq1976.00472425000500040028x.

Rudd, John W. M. “Sources of Methyl Mercury to Freshwater Ecosystems: A Review.” *Water, Air, and Soil Pollution* 80, no. 1 (February 1, 1995): 697–713. https://doi.org/10.1007/BF01189722.

San Francisco Bay Water Quality Control, California State Coastal Conservancy, Stillwater Sciences, Dietrich, W. “ Board “Napa River watershed Limiting Factors Analysis” Final Technical Report. www.waterboards.ca.gov/rwqcb2/water_issues/available_documents/technicalreport.pdf.“Htt

ps://Www.Waterboards.ca.Gov/Rwqcb2/Water_issues/Available_documents/Technicalreport.Pdf." 14, June 2002. Accessed April 3, 2024.

Sansalone, J.J., Cristina, C.M., 2004. First flush concepts for suspended and dissolved solids in small impervious watersheds. Journal of Environmental Engineering ASCE 130 (11), 1301–1314. https://doi.org/10.1061/(ASCE)0733-9372(2004)130:11(1301)

Schaefer, Jeffra K., Sara S. Rocks, Wang Zheng, Liyuan Liang, Baohua Gu, and François M. M. Morel. "Active Transport, Substrate Specificity, and Methylation of Hg(II) in Anaerobic Bacteria." *Proceedings of the National Academy of Sciences* 108, no. 21 (May 24, 2011): 8714–19. https://doi.org/10.1073/pnas.1105781108.

Selin, Noelle E. "Global Biogeochemical Cycling of Mercury: A Review." *Annual Review of Environment and Resources* 34, no. 1 (November 1, 2009): 43–63. https://doi.org/10.1146/annurev.environ.051308.084314.

Stoken, Olivia M., Ami L. Riscassi, and Todd M. Scanlon. "Association of Dissolved Mercury with Dissolved Organic Carbon in U.S. Rivers and Streams: The Role of Watershed Soil Organic Carbon." *Water Resources Research* 52, no. 4 (April 2016): 3040–51. https://doi.org/10.1002/2015WR017849.

Tanner, K. Christy, Lisamarie Windham-Myers, Jacob A. Fleck, Kenneth W. Tate, Stephen A. McCord, and Bruce A. Linquist. "The Contribution of Rice Agriculture to Methylmercury in Surface Waters: A Review of Data from the Sacramento Valley, California." *Journal of Environmental Quality* 46, no. 1 (2017): 133–42. https://doi.org/10.2134/jeq2016.07.0262.

Tsui, Martin Tsz Ki, Jacques C. Finlay, and Edward A. Nater. "Mercury Bioaccumulation in a Stream Network." *Environmental Science & Technology* 43, no. 18 (September 15, 2009): 7016–22. https://doi.org/10.1021/es901525w.

Tsui, Martin Tsz Ki, Jacques C. Finlay, Steven J. Balogh, and Yabing H. Nollet. "In Situ Production of Methylmercury within a Stream Channel in Northern California." *Environmental Science & Technology* 44, no. 18 (September 15, 2010): 6998–7004. https://doi.org/10.1021/es101374y.

United Nations Environment Programme (2013). *Global Mercury Assessment 2013: Sources, emissions, releases, and environmental transport*. https://wedocs.unep.org/20.500.11822/7984. https://wedocs.unep.org/xmlui/handle/20.500.11822/7984. Date accessed 5/1/2024.

United States Environmental Protection Agency. "Fish and Shellfish Advisories and Safe Eating Guidelines." www.epa.gov/choose-fish-and-shellfish-wisely/fish-and-shellfish-advisories-and-safe-eating-guidelines, updated December 28, 2023. Date accessed 5/10/2024.

Wagner, David L., George J. Saucedo, Kevin B. Clahan, Robert J. Fleck, Victoria E. Langenheim, Robert J. McLaughlin, Andrei M. Sarna-Wojcicki, James R. Allen, Alan L. Deino; Geology, geochronology, and paleogeography of the southern Sonoma volcanic field and adjacent areas, northern San Francisco Bay region, California. *Geosphere* 2011;; 7 (3): 658–683. doi: https://doi.org/10.1130/GES00626.1

Wang, Yuqin, Jiang Liu, Van Liem-Nguyen, Shanyi Tian, Siqi Zhang, Dingyong Wang, and Tao Jiang. “Binding Strength of Mercury (II) to Different Dissolved Organic Matter: The Roles of DOM Properties and Sources.” *Science of The Total Environment* 807 (February 10, 2022): 150979. https://doi.org/10.1016/j.scitotenv.2021.150979.

Weiss, P., Eve-Lyn S. Hinckley, Calvin, J., “Methylation Rates in Vineyard Soils in Napa Valley Watershed.” Unpublished.

Yu, Ri-Qing, John R. Reinfelder, Mark E. Hines, and Tamar Barkay. “Mercury Methylation by the Methanogen Methanospirillum Hungatei.” *Applied and Environmental Microbiology* 79, no. 20 (October 15, 2013): 6325–30. https://doi.org/10.1128/AEM.01556-13.

Yu, Ri-Qing, and Tamar Barkay. “Microbial Mercury Transformations: Molecules, Functions and Organisms.” In *Advances in Applied Microbiology*, 118:31–90. Elsevier, 2022. https://doi.org/10.1016/bs.aambs.2022.03.001.